Supplementary material

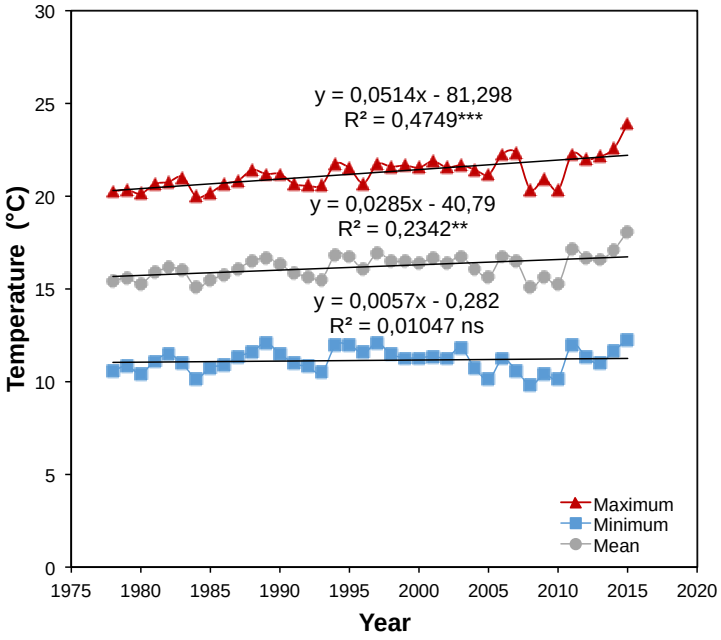

Figure S1. Annual temperature trends (mean, maximum and minimum) in Reus Airport during the period 1978-2015. Levels of significance: ns (not significant); * (p<0.05); **(p<0.01); ***(p<0.001).

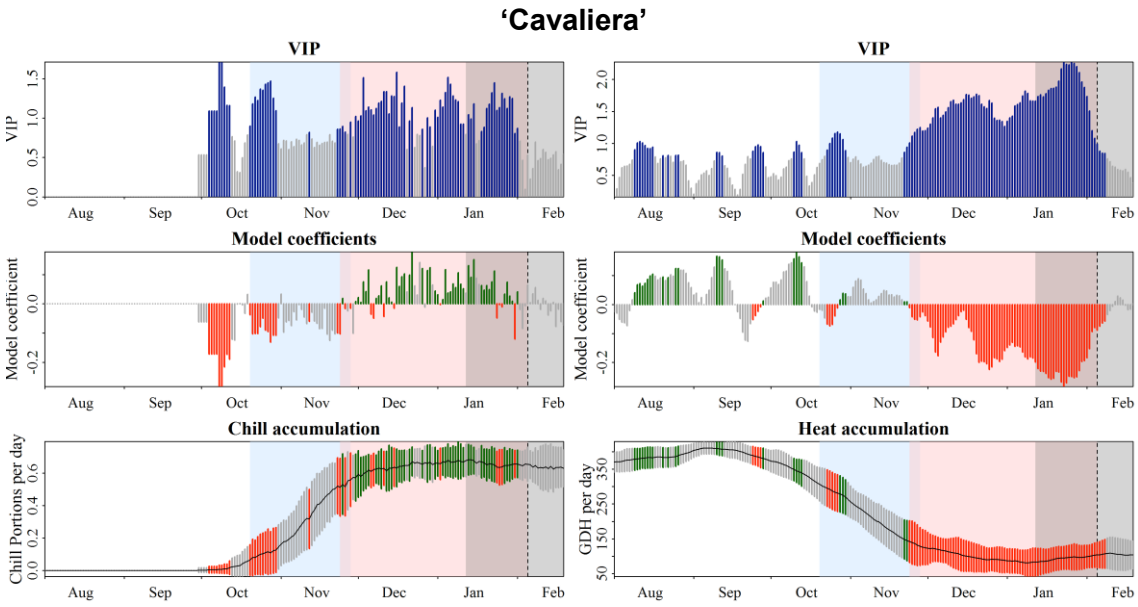

Figure S2. Results obtained from the PLS regression analysis between blooming dates and daily mean chill and heat accumulation for 'Cavaliera' in Mas de Bover using the Dynamic Model and the GDH Model. Chilling phase on the left, forcing phase on the right. Top: VIP values (Variable Importance of the Projection). Middle: standardized coefficients of the PLS model. Bottom: daily mean chill/heat accumulation in Chill Portions and Growing Degree Hour (GDH) units, left and right respectively: the length of the bars in this panel indicates the standard deviation of the daily chill/heat accumulation. For all panels, coloured bars indicate VIP≥ 0.8; red bars, the standardized coefficients of the model are negative indicating that chill or heat accumulated in that day (left and right panel, respectively) result in an advancement of the flowering date; for green bars, coefficients are positive an indicate flowering date delay. Blue and pink background colours emphasize the delineated chilling and forcing phases, background grey represents the period when flowering occurs along the years studied, and the dotted line marks the median date of all the blooming dates recorded from 1979 to 2015.

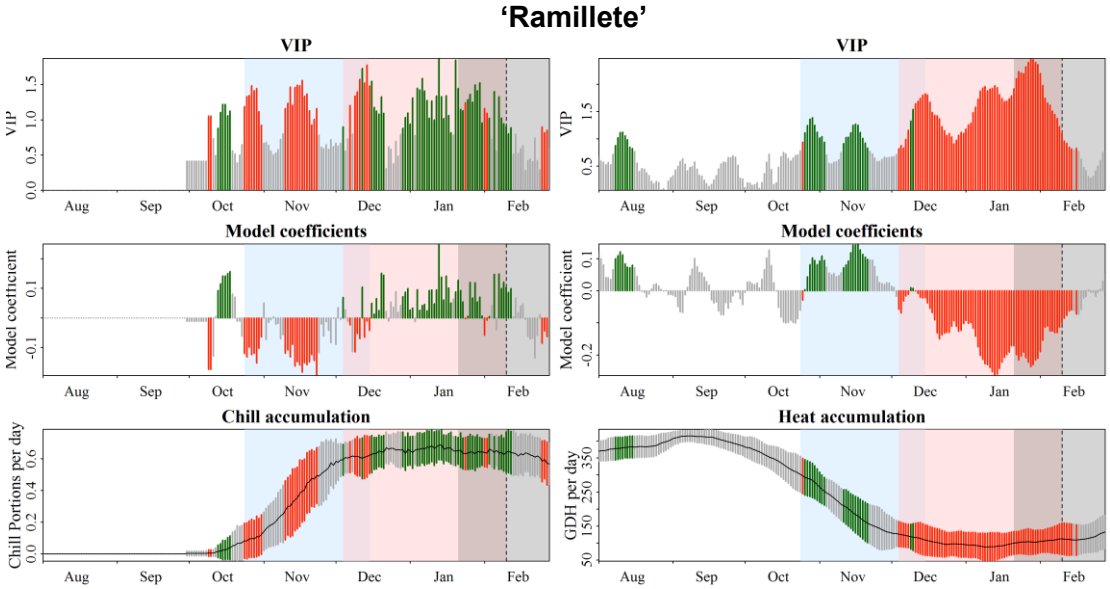

Figure S3. Results obtained from the PLS regression analysis between blooming dates and daily mean chill and heat accumulation for 'Ramillete' in Mas de Bover using the Dynamic Model and the GDH Model. See caption in Figure S2 for full explanation.

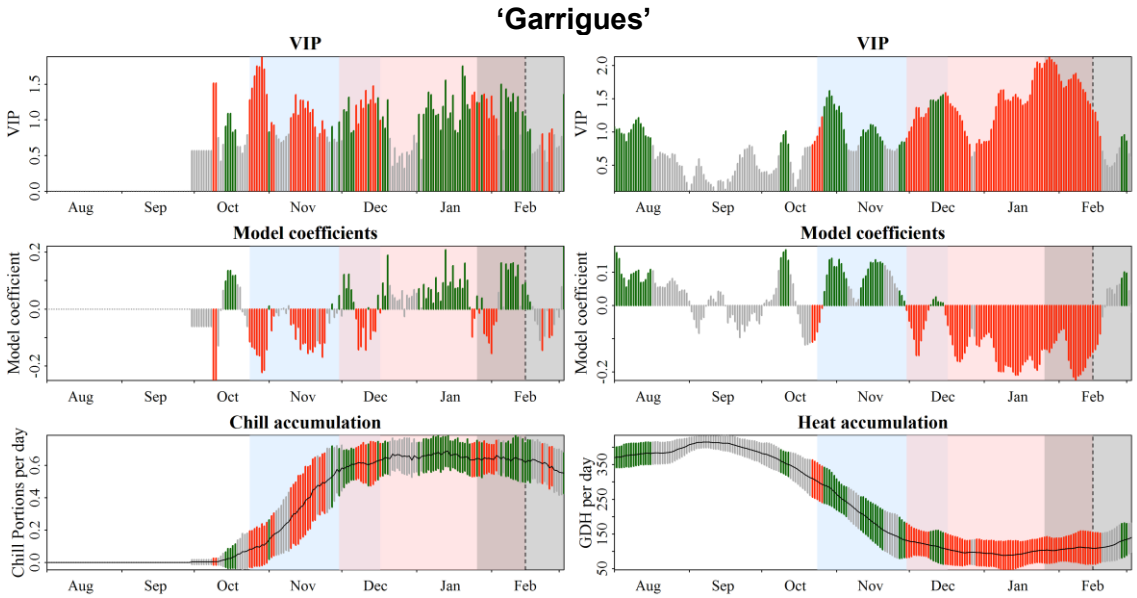

Figure S4. Results obtained from the PLS regression analysis between blooming dates and daily mean chill and heat accumulation for 'Garrigues' in Mas de Bover using the Dynamic Model and the GDH Model. See caption in Figure S2 for full explanation.

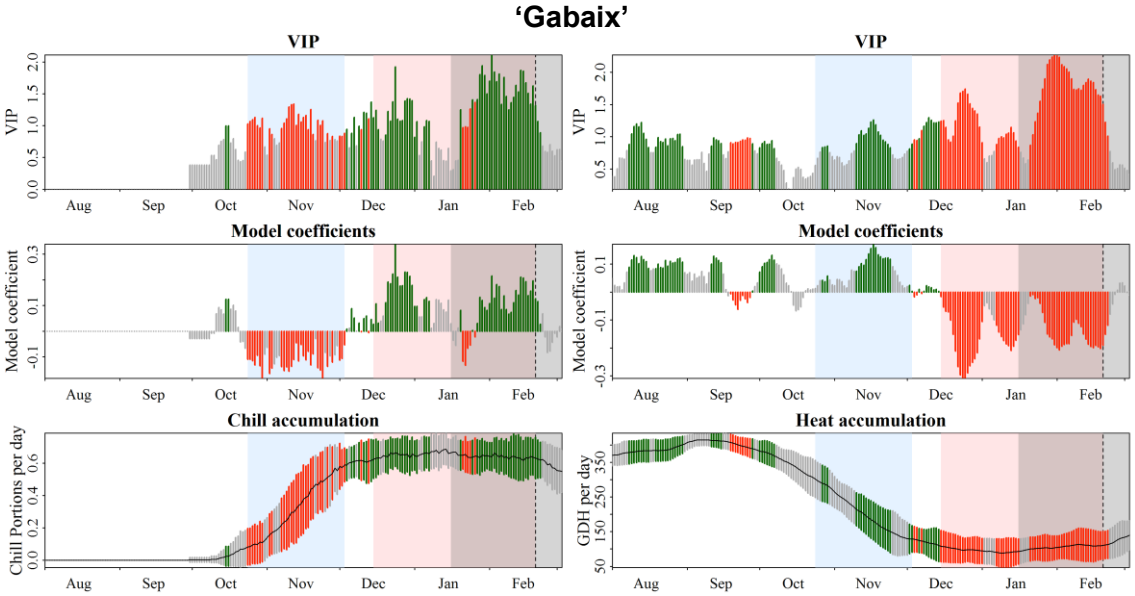

Figure S5. Results obtained from the PLS regression analysis between blooming dates and daily mean chill and heat accumulation for 'Gabaix' in Mas de Bover using the Dynamic Model and the GDH Model. See caption in Figure S2 for full explanation.

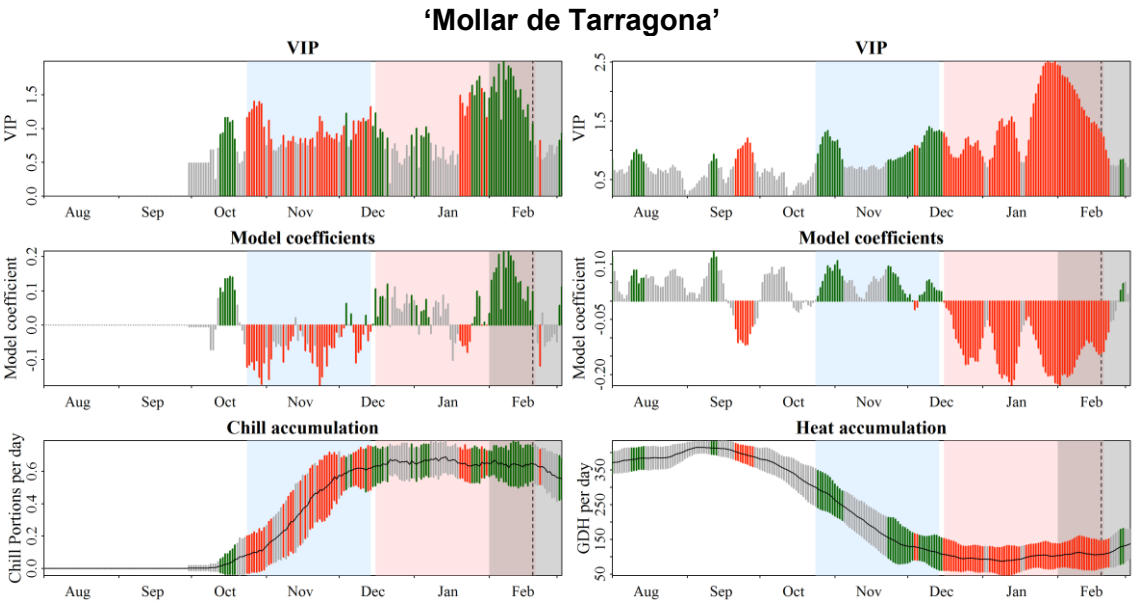

Figure S6. Results obtained from the PLS regression analysis between blooming dates and daily mean chill and heat accumulation for 'Mollar de Tarragona' in Mas de Bover using the Dynamic Model and the GDH Model. See caption in Figure S2 for full explanation.

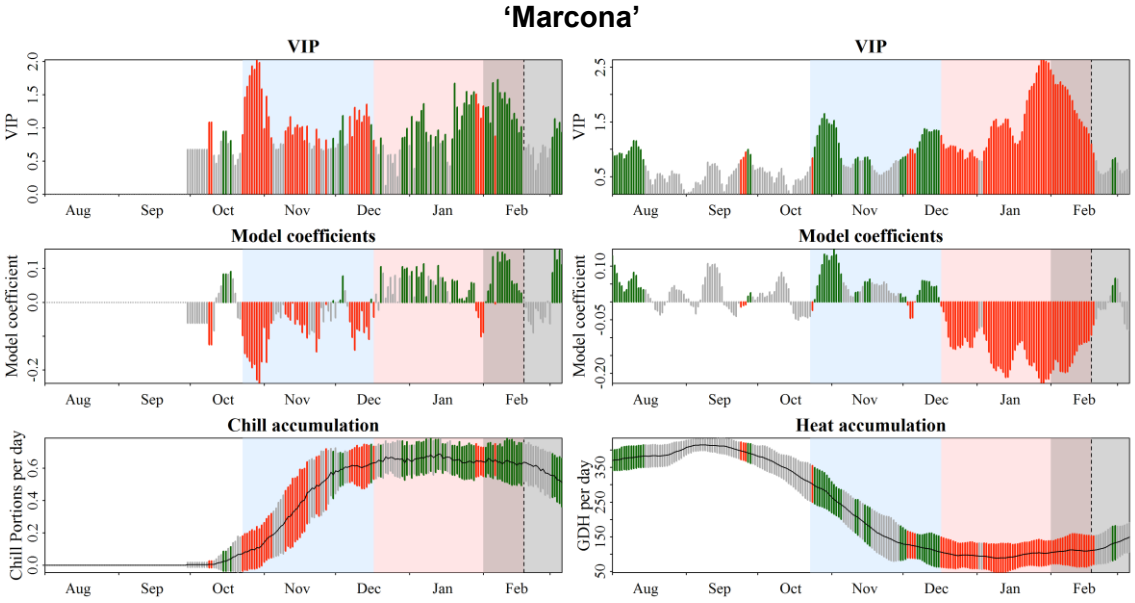

Figure S7. Results obtained from the PLS regression analysis between blooming dates and daily mean chill and heat accumulation for Marcona in Mas de Bover using the Dynamic Model and the GDH Model. See caption in Figure S2 for full explanation.

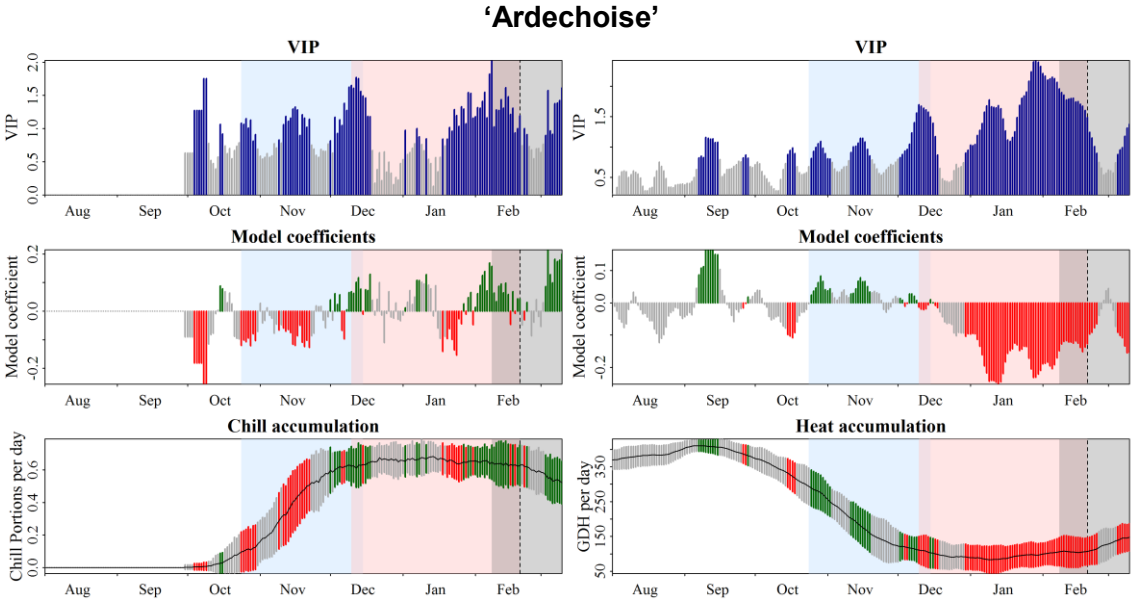

Figure S8. Results obtained from the PLS regression analysis between blooming dates and daily mean chill and heat accumulation for 'Ardechoise' in Mas de Bover using the Dynamic Model and the GDH Model. See caption in Figure S2 for full explanation.

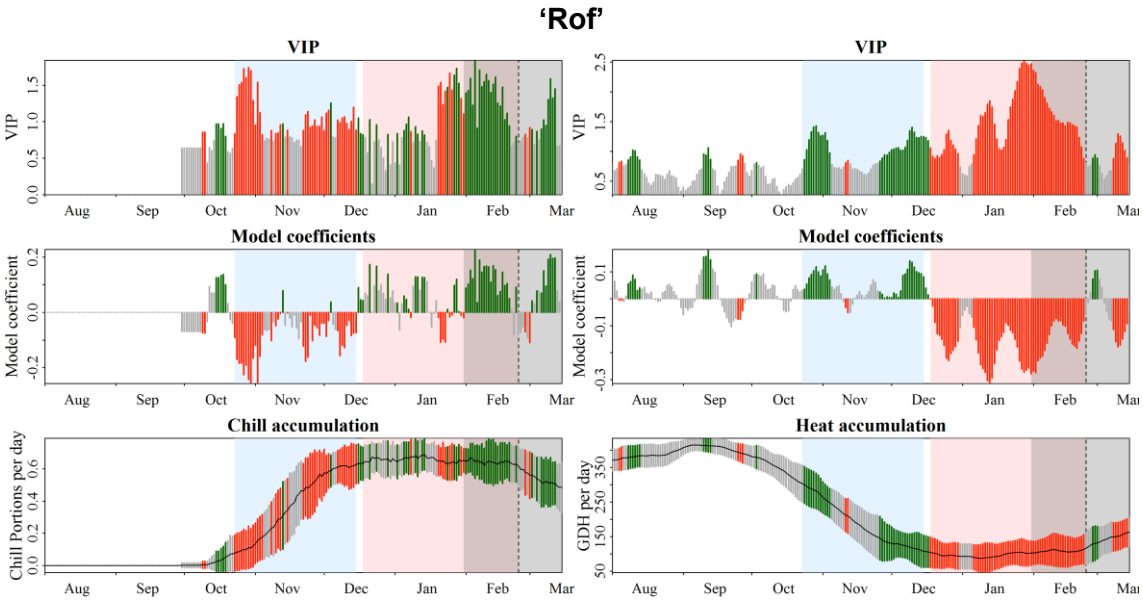

Figure S9. Results obtained from the PLS regression analysis between blooming dates and daily mean chill and heat accumulation for 'Rof' in Mas de Bover using the Dynamic Model and the GDH Model. See caption in Figure S2 for full explanation.

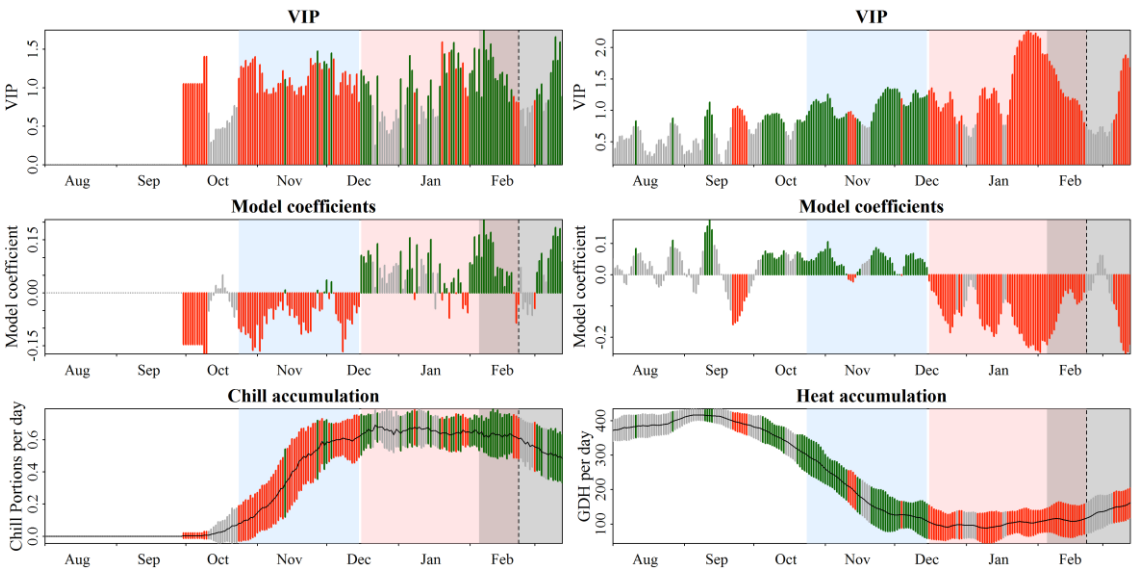

Figure S10. Results obtained from the PLS regression analysis between blooming dates and daily mean chill and heat accumulation for 'Alicante' in Mas de Bover using the Dynamic Model and the GDH Model. See caption in Figure S2 for full explanation.

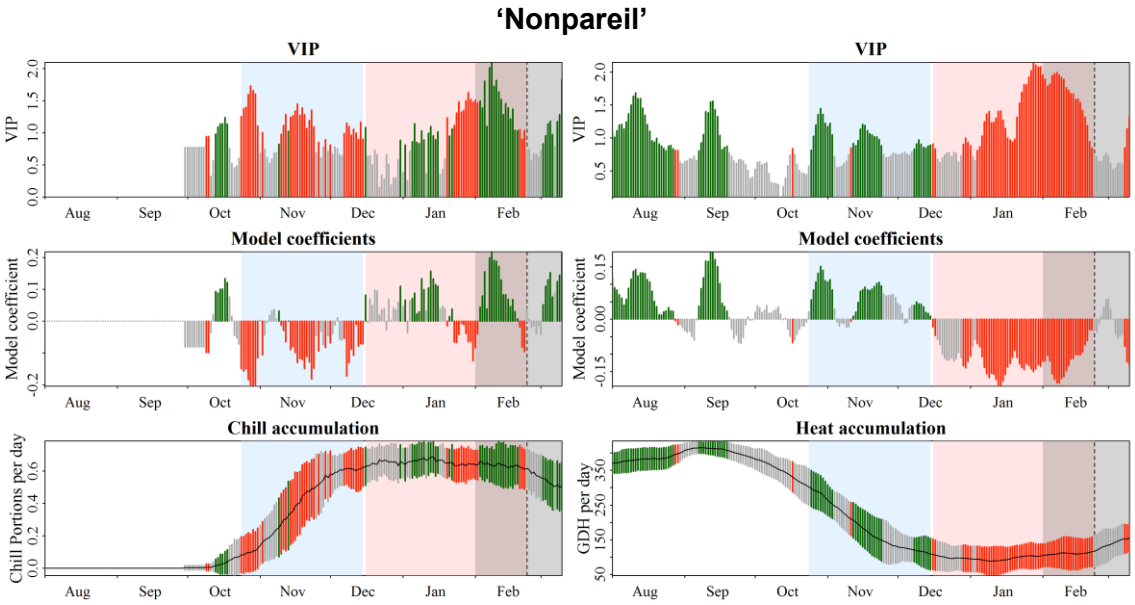

Figure S11. Results obtained from the PLS regression analysis between blooming dates and daily mean chill and heat accumulation for 'Nonpareil' in Mas de Bover using the Dynamic Model and the GDH Model. See caption in Figure S2 for full explanation.

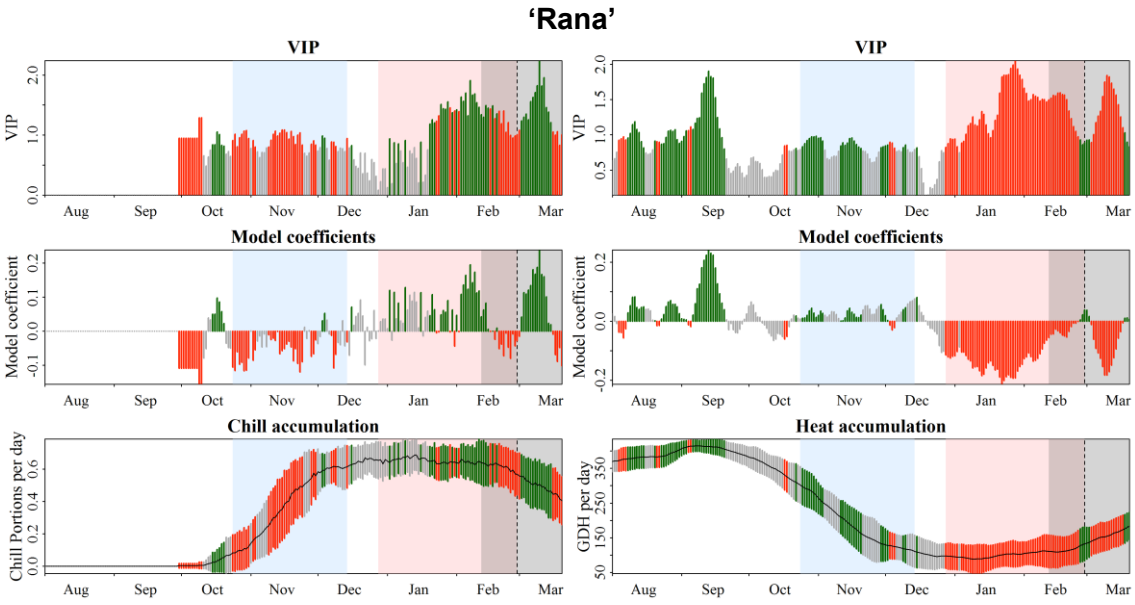

Figure S12. Results obtained from the PLS regression analysis between blooming dates and daily mean chill and heat accumulation for 'Rana' in Mas de Bover using the Dynamic Model and the GDH Model. See caption in Figure S2 for full explanation.

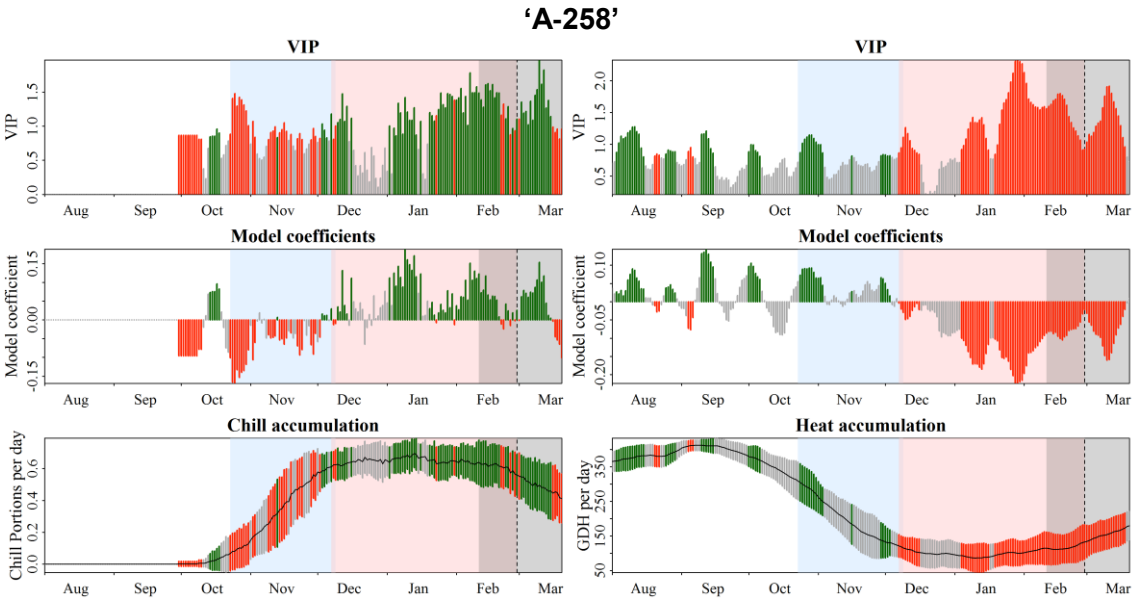

Figure S13. Results obtained from the PLS regression analysis between blooming dates and daily mean chill and heat accumulation for 'A-258' in Mas de Bover using the Dynamic Model and the GDH Model. See caption in Figure S2 for full explanation.

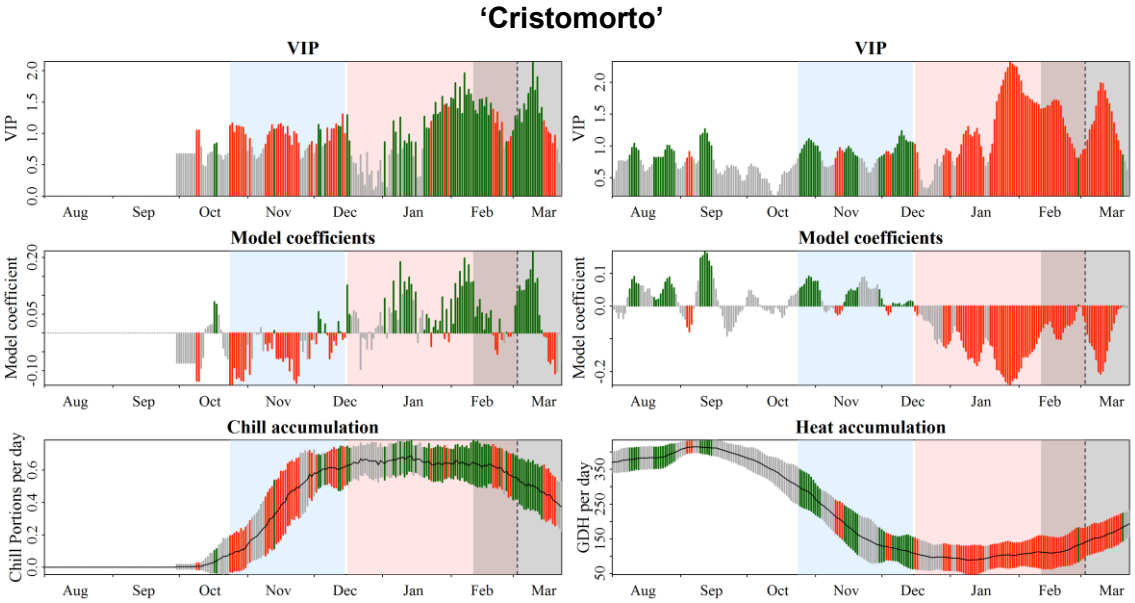

Figure S14. Results obtained from the PLS regression analysis between blooming dates and daily mean chill and heat accumulation for 'Cristomorto' in Mas de Bover using the Dynamic Model and the GDH Model. See caption in Figure S2 for full explanation.

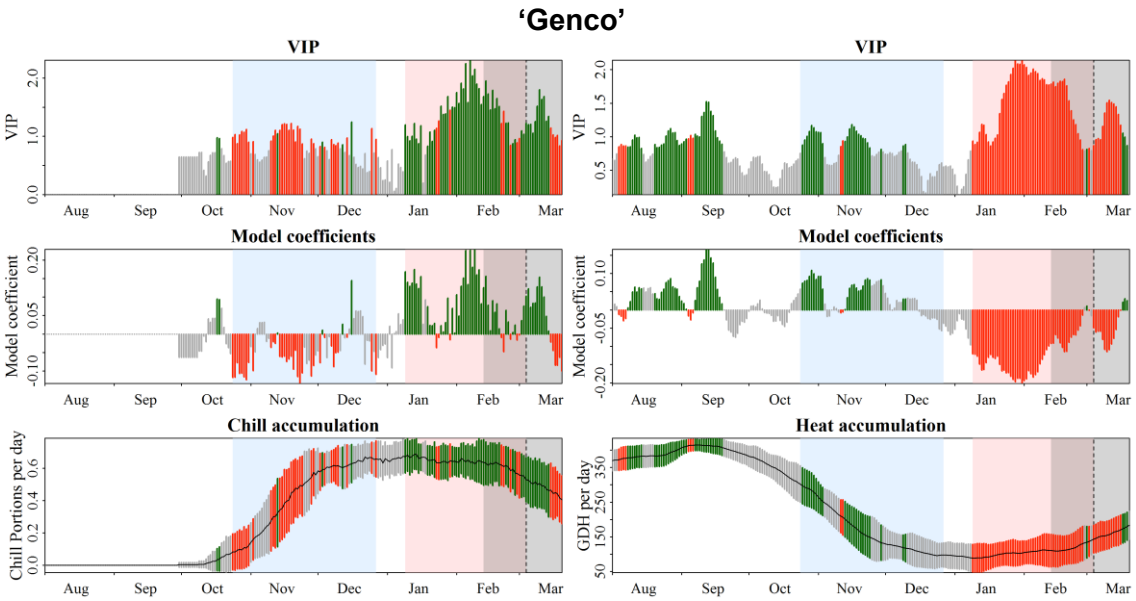

Figure S15. Results obtained from the PLS regression analysis between blooming dates and daily mean chill and heat accumulation for 'Genco' in Mas de Bover using the Dynamic Model and the GDH Model. See caption in Figure S2 for full explanation.

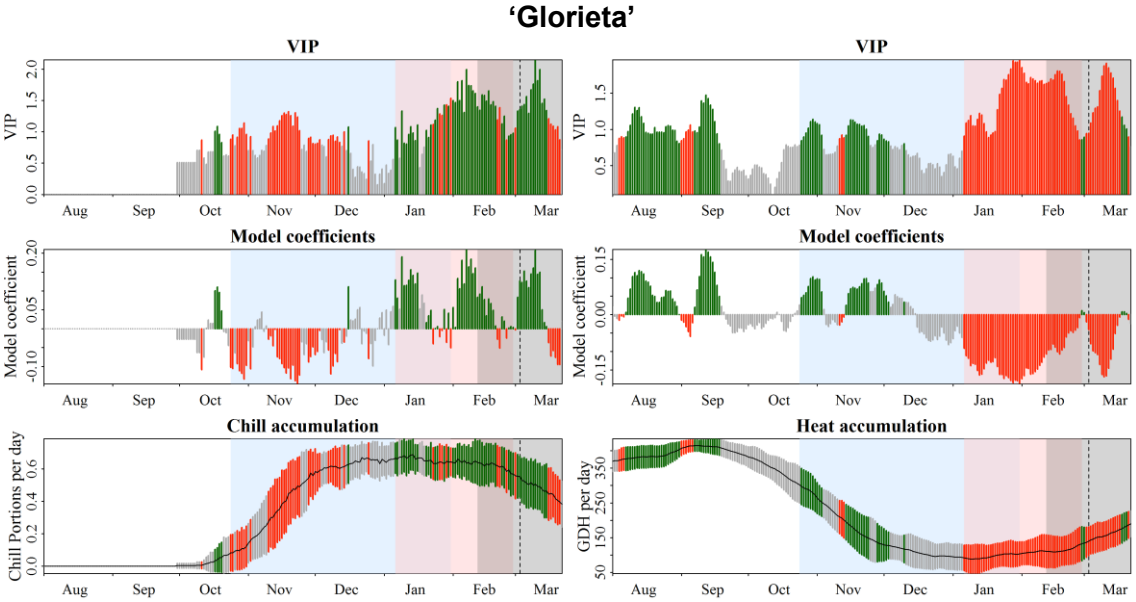

Figure S16. Results obtained from the PLS regression analysis between blooming dates and daily mean chill and heat accumulation for 'Glorieta' in Mas de Bover using the Dynamic Model and the GDH Model. See caption in Figure S2 for full explanation.

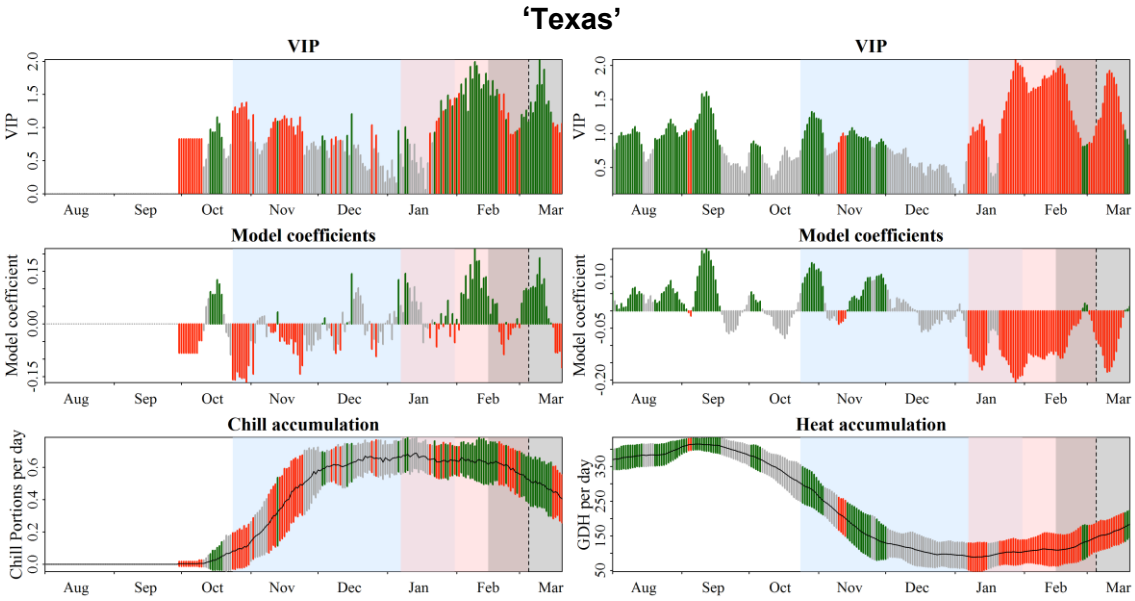

Figure S17. Results obtained from the PLS regression analysis between blooming dates and daily mean chill and heat accumulation for 'Texas' in Mas de Bover using the Dynamic Model and the GDH Model. See caption in Figure S2 for full explanation.

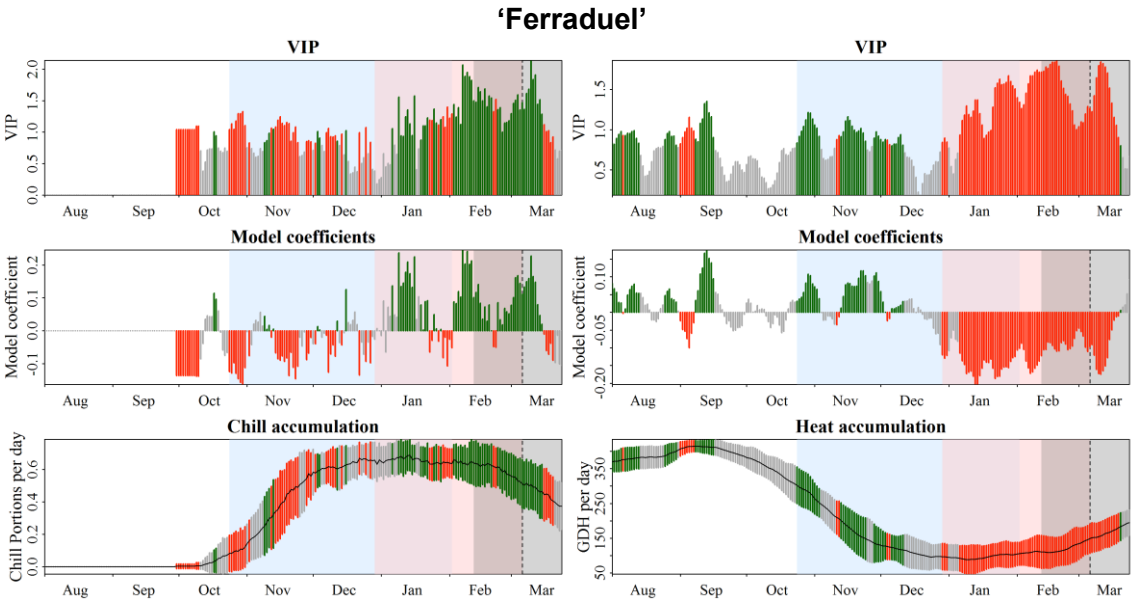

Figure S18. Results obtained from the PLS regression analysis between blooming dates and daily mean chill and heat accumulation for 'Ferraduel' in Mas de Bover using the Dynamic Model and the GDH Model. See caption in Figure S2 for full explanation.

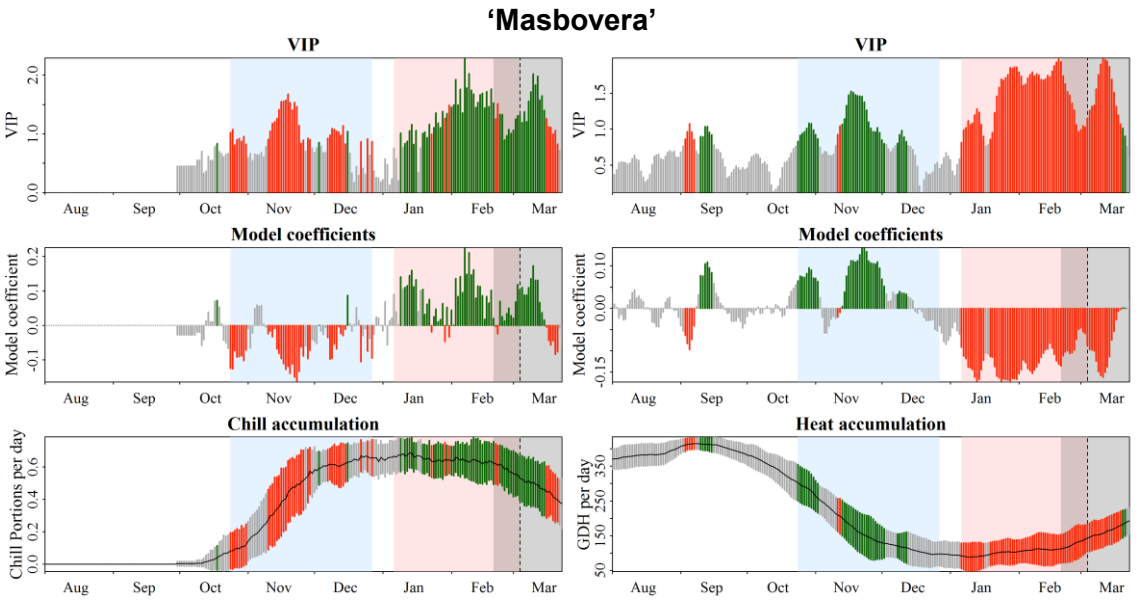

Figure S19. Results obtained from the PLS regression analysis between blooming dates and daily mean chill and heat accumulation for Masbovera in Mas de Bover using the Dynamic Model and the GDH Model. See caption in Figure S2 for full explanation.

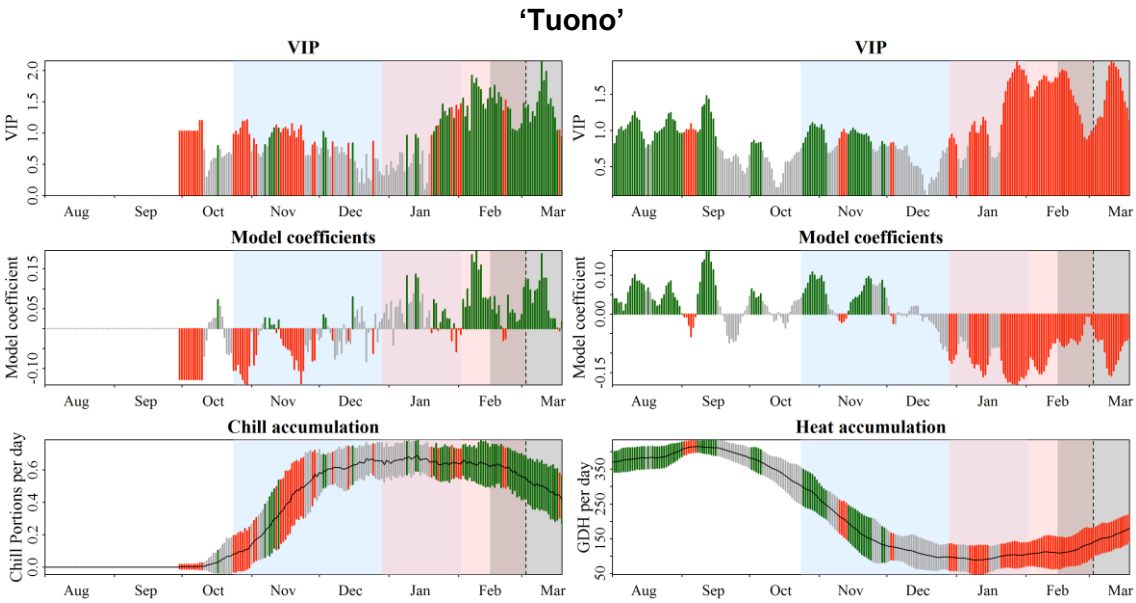

Figure S20. Results obtained from the PLS regression analysis between blooming dates and daily mean chill and heat accumulation for 'Tuono' in Mas de Bover using the Dynamic Model and the GDH Model. See caption in Figure S2 for full explanation.

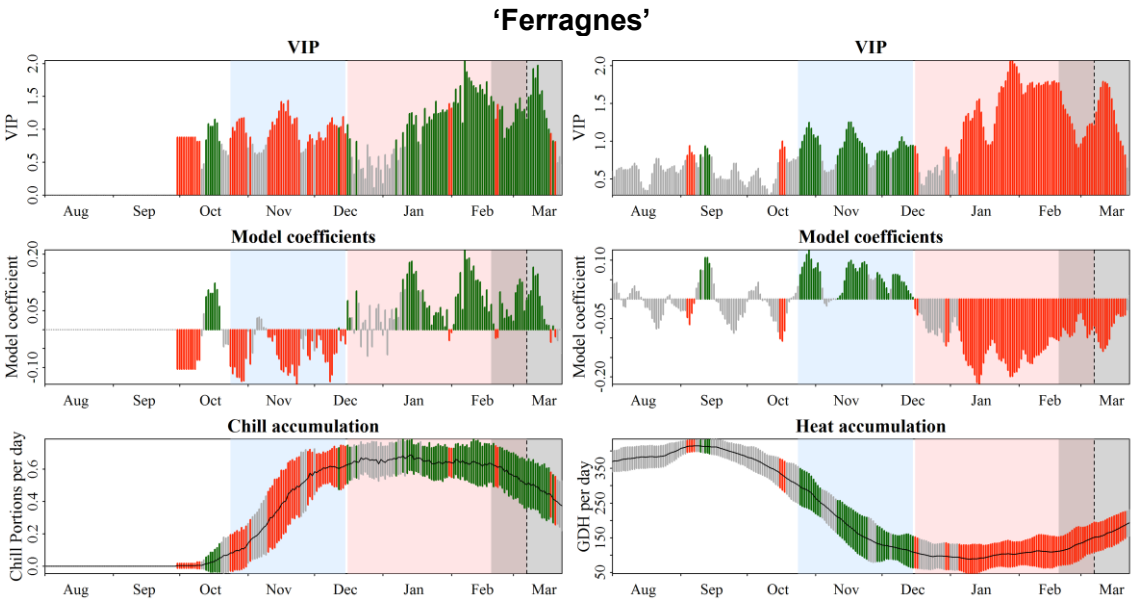

Figure S21. Results obtained from the PLS regression analysis between blooming dates and daily mean chill and heat accumulation for 'Ferragnes' in Mas de Bover using the Dynamic Model and the GDH Model. See caption in Figure S2 for full explanation.

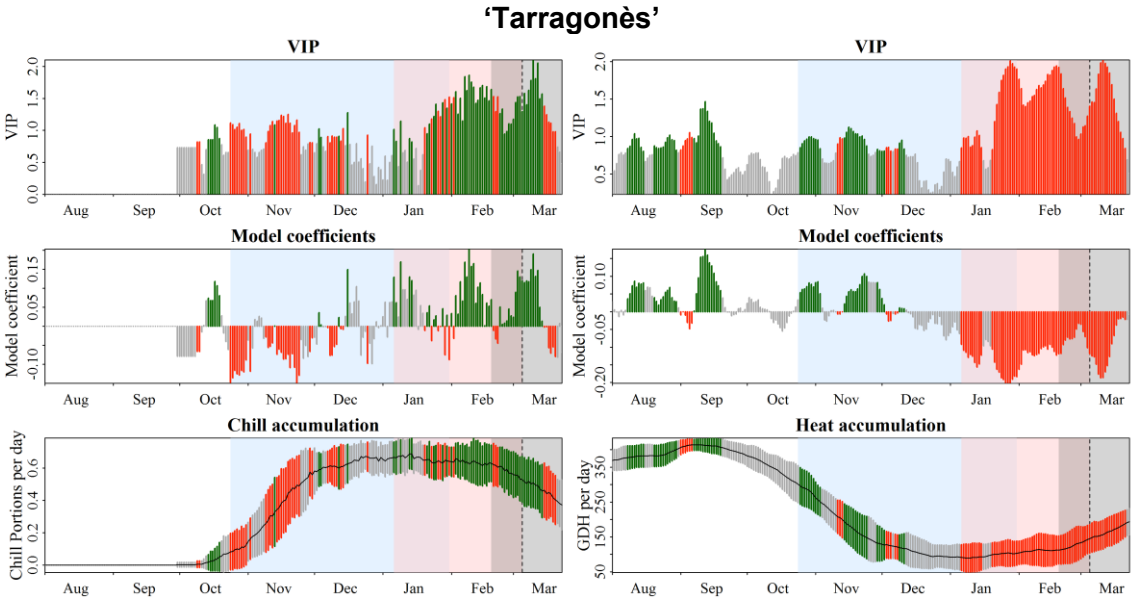

Figure S22. Results obtained from the PLS regression analysis between blooming dates and daily mean chill and heat accumulation for 'Tarragonès' in Mas de Bover using the Dynamic Model and the GDH Model. See caption in Figure S2 for full explanation.

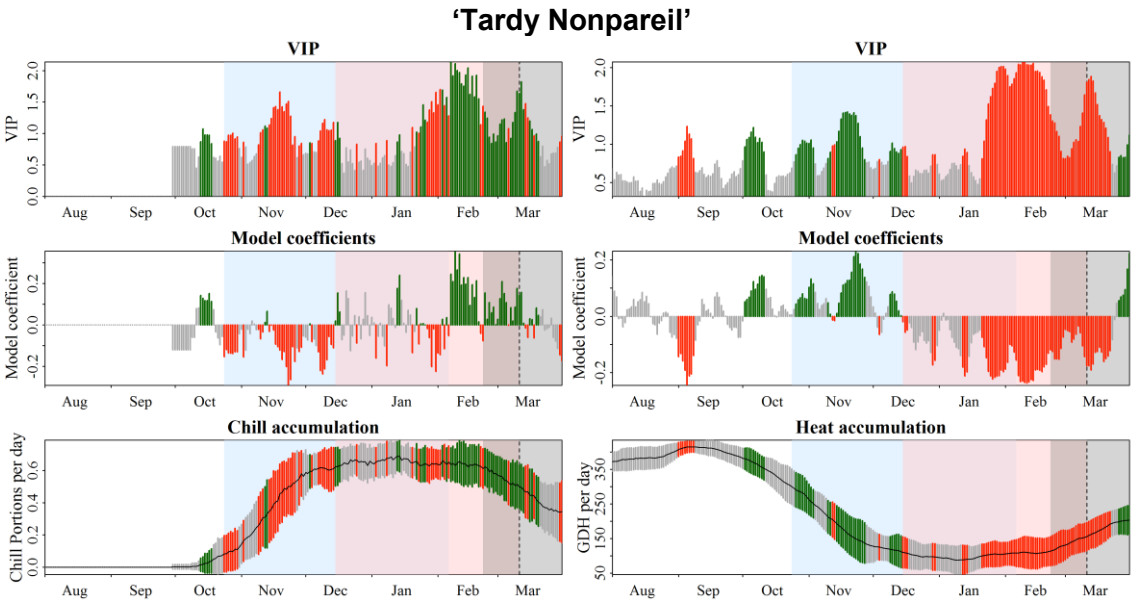

Figure S23. Results obtained from the PLS regression analysis between blooming dates and daily mean chill and heat accumulation for 'Tardy Nonpareil' in Mas de Bover using the Dynamic Model and the GDH Model. See caption in Figure S2 for full explanation.

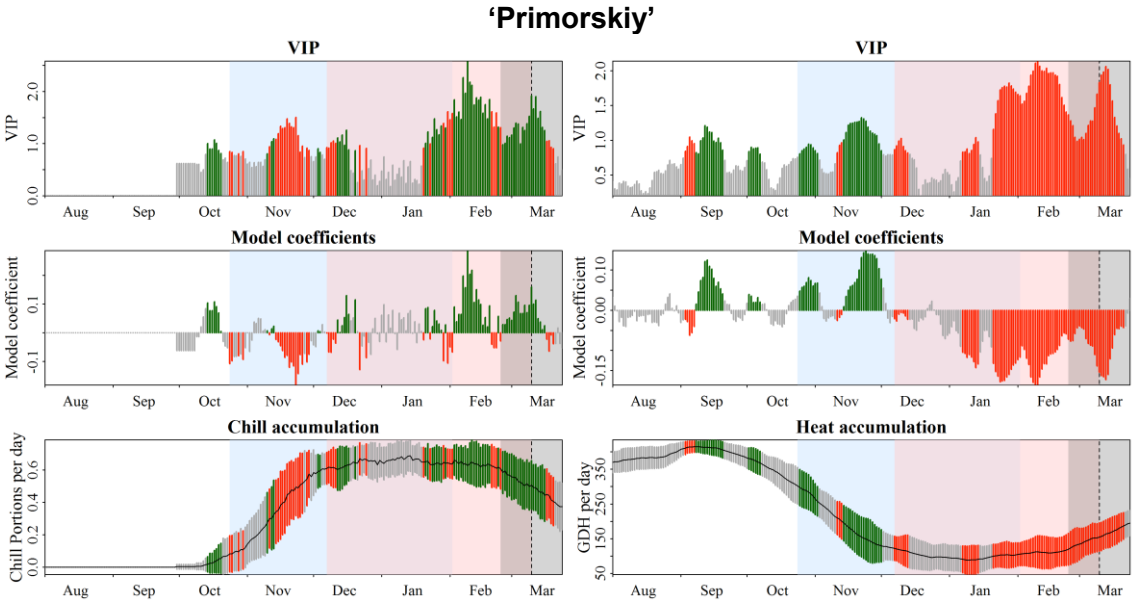

Figure S24. Results obtained from the PLS regression analysis between blooming dates and daily mean chill and heat accumulation for 'Primorskiy' in Mas de Bover using the Dynamic Model and the GDH Model. See caption in Figure S2 for full explanation.

‘Pink Lady’

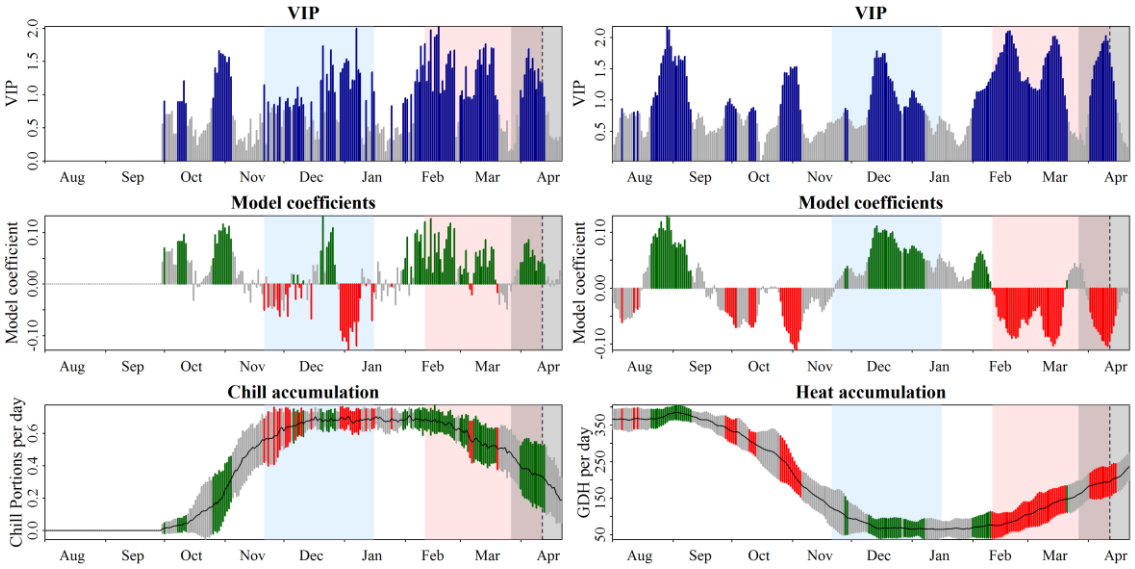

Figure S25. Results obtained from the PLS regression analysis between blooming dates and daily mean chill and heat accumulation for ‘Pink Lady’ in Mas Badia using the Dynamic Model and the GDH Model. Chilling phase on the left, forcing phase on the right. Top: VIP values (Variable Importance of the Projection). Middle: standardized coeficients of the PLS model. Bottom: daily mean chill/heat accumulation in Chill Portions and Growing Degree Hour (GDH) units, left and right respectively: the length of the bars in this panel indicates the standard deviation of the daily chill/heat accumulation. For all panels, coloured bars indicate VIP≥ 0.8; red bars, the standardized coeficients of the model are negative indicating that chill or heat accumulated in that day (left and right pannel, respectively) result in an advancement of the flowering date; for green bars, coeficients are positive an indicate flowering date delay. Blue and pink background colours emphasize the delineated chilling and forcing phases, background grey represents the period when flowering occurs along the years studied, and the dotted line marks the median date of all the blooming dates recorded from 1992 to 2018.

‘Brookfield Gala’

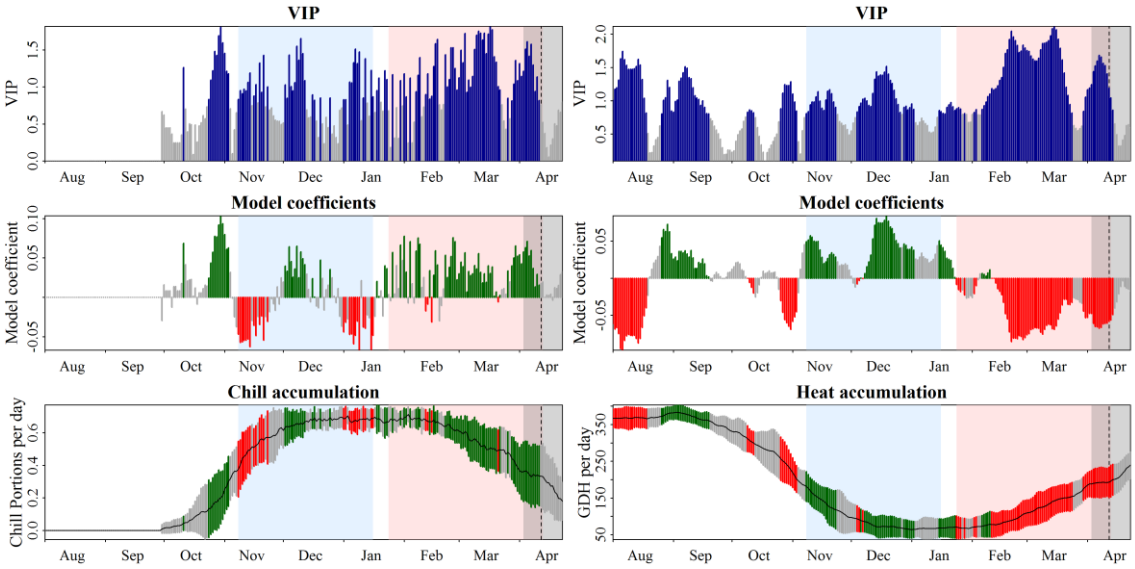

Figure S26. Results obtained from the PLS regression analysis between blooming dates and daily mean chill and heat accumulation for ‘Brookfield Gala’ in Mas Badia using the Dynamic Model and the GDH Model. See caption in Figure S25 for full explanation.

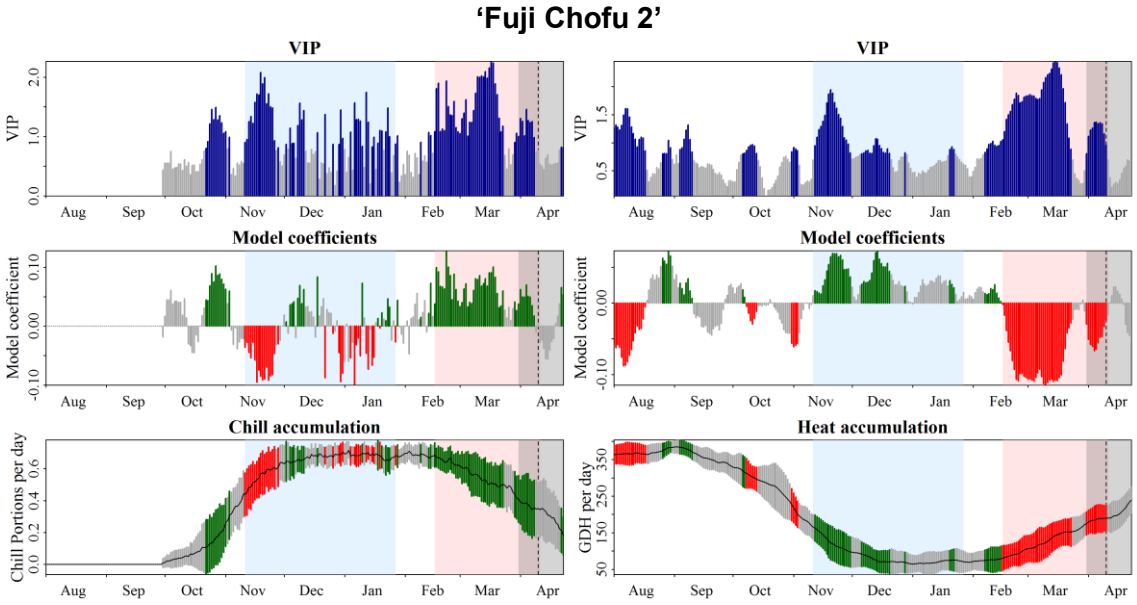

Figure S27. Results obtained from the PLS regression analysis between blooming dates and daily mean chill and heat accumulation for 'Fuji Chofu 2' in Mas Badia using the Dynamic Model and the GDH Model. See caption in Figure S25 for full explanation.

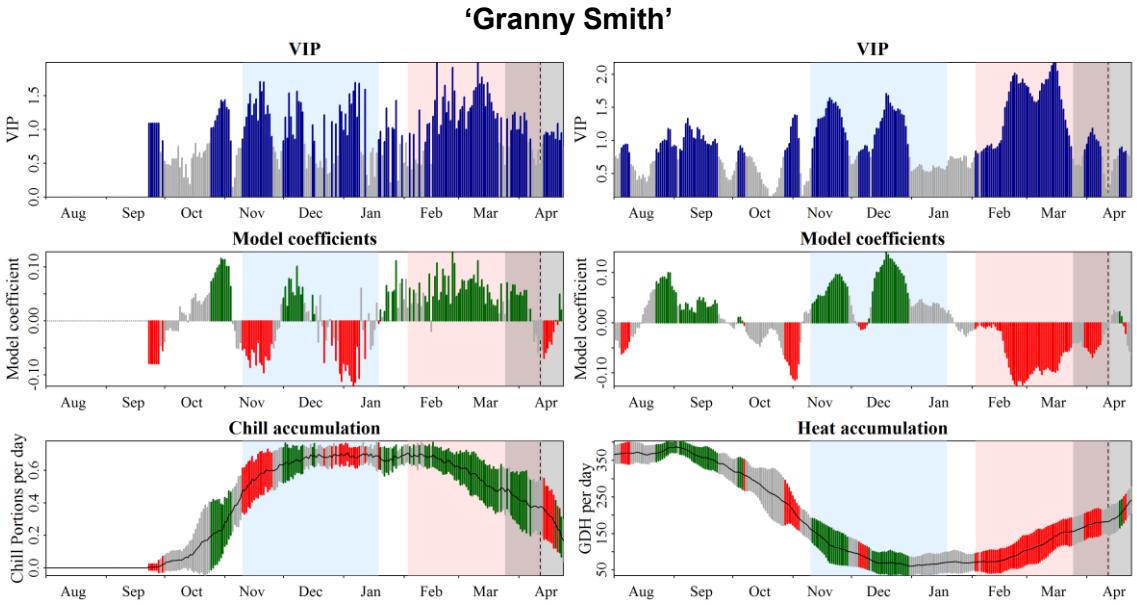

Figure S28. Results obtained from the PLS regression analysis between blooming dates and daily mean chill and heat accumulation for 'Granny Smith' in Mas Badia using the Dynamic Model and the GDH Model. See caption in Figure S25 for full explanation.

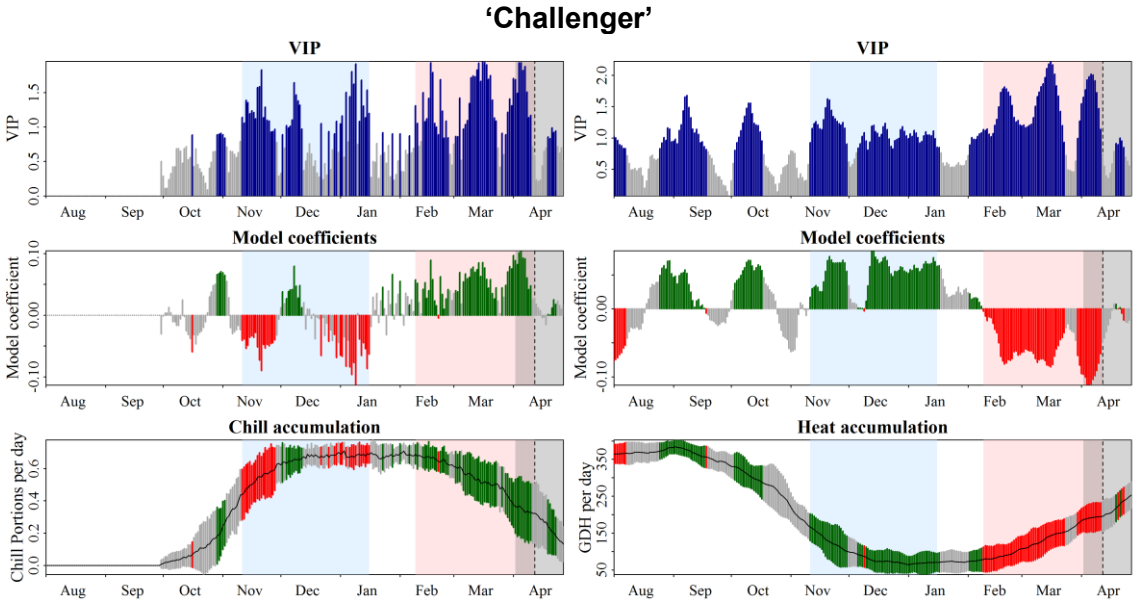

Figure S29. Results obtained from the PLS regression analysis between blooming dates and daily mean chill and heat accumulation for ‘Challenger’ in Mas Badia using the Dynamic Model and the GDH Model. See caption in Figure S25 for full explanation.

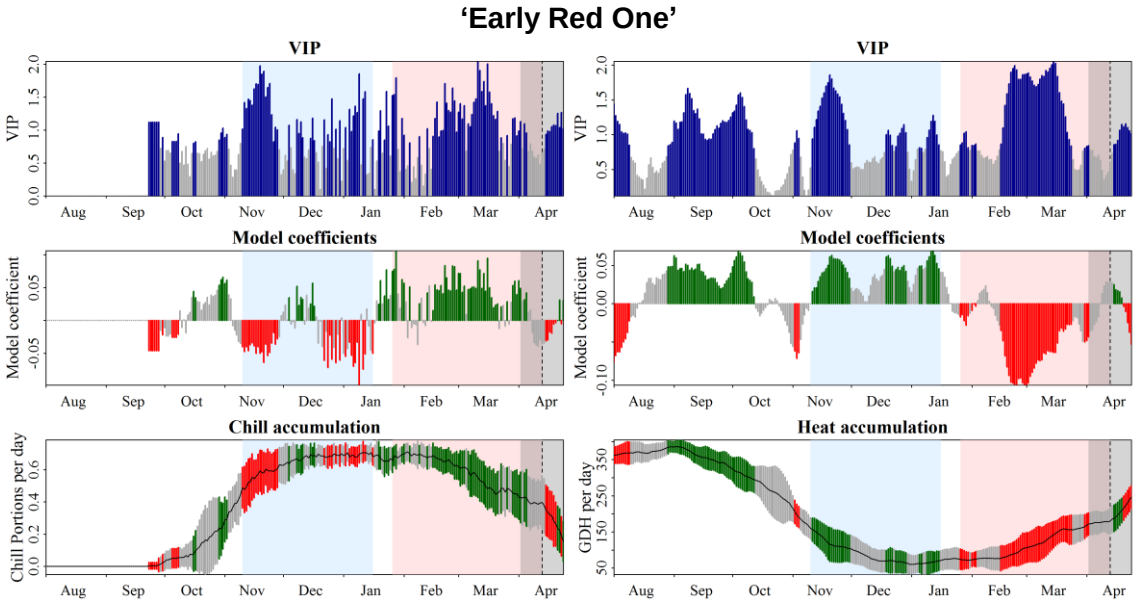

Figure S30. Results obtained from the PLS regression analysis between blooming dates and daily mean chill and heat accumulation for ‘Early Red One’ in Mas Badia using the Dynamic Model and the GDH Model. See caption in Figure S25 for full explanation.

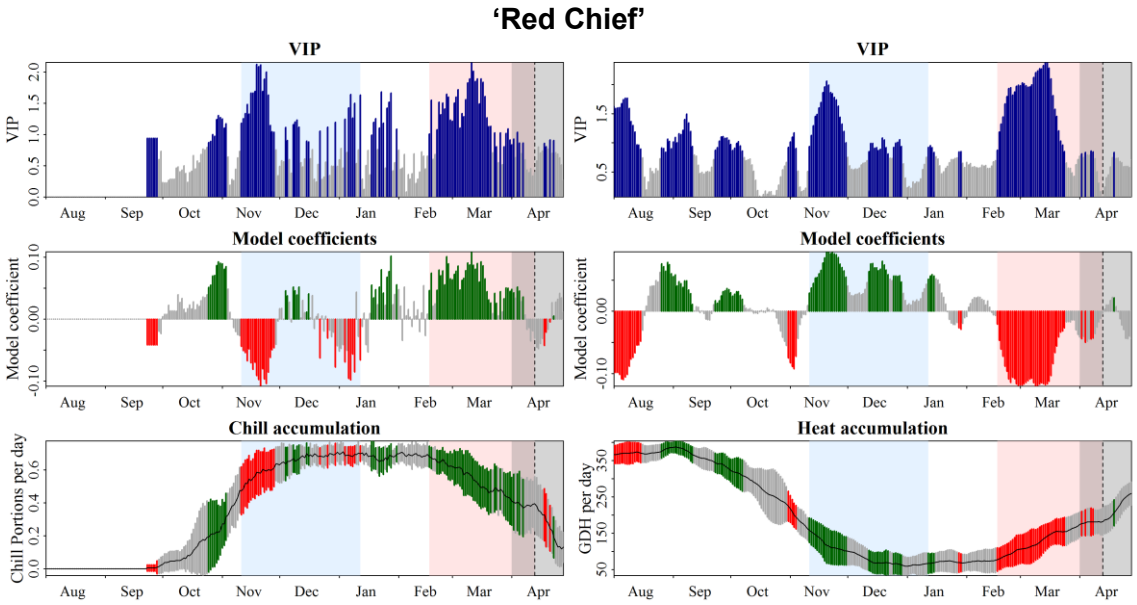

Figure S31. Results obtained from the PLS regression analysis between blooming dates and daily mean chill and heat accumulation for ‘Red Chief’ in Mas Badia using the Dynamic Model and the GDH Model. See caption in Figure S25 for full explanation.

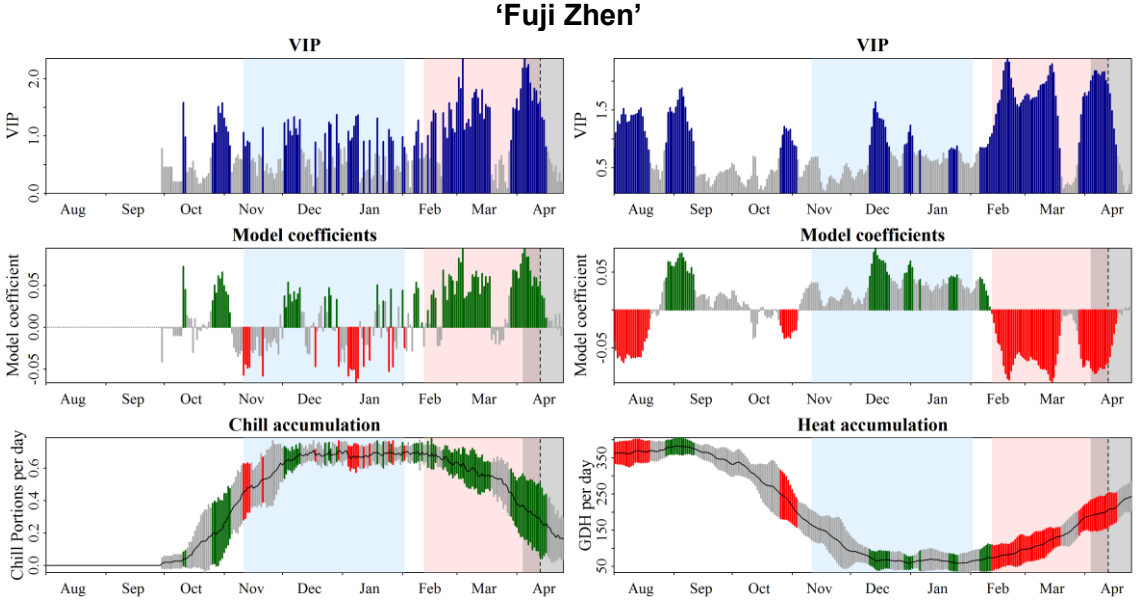

Figure S32. Results obtained from the PLS regression analysis between blooming dates and daily mean chill and heat accumulation for ‘Fuji Zhen’ in Mas Badia using the Dynamic Model and the GDH Model. See caption in Figure S25 for full explanation.

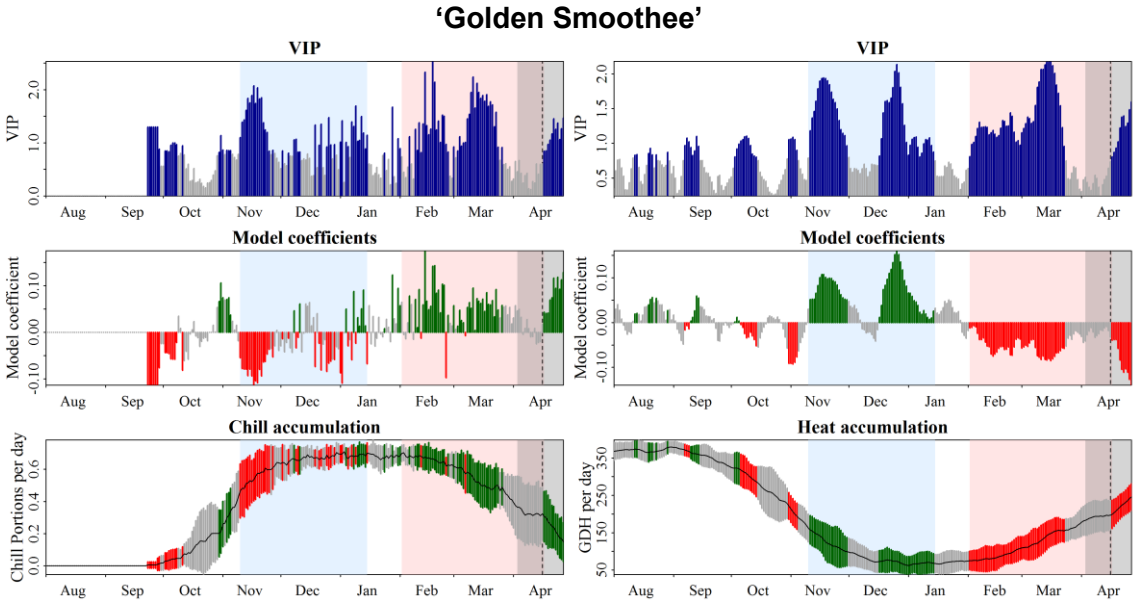

Figure S33. Results obtained from the PLS regression analysis between blooming dates and daily mean chill and heat accumulation for 'Golden Smoothee' in Mas Badia using the Dynamic Model and the GDH Model. See caption in Figure S25 for full explanation.

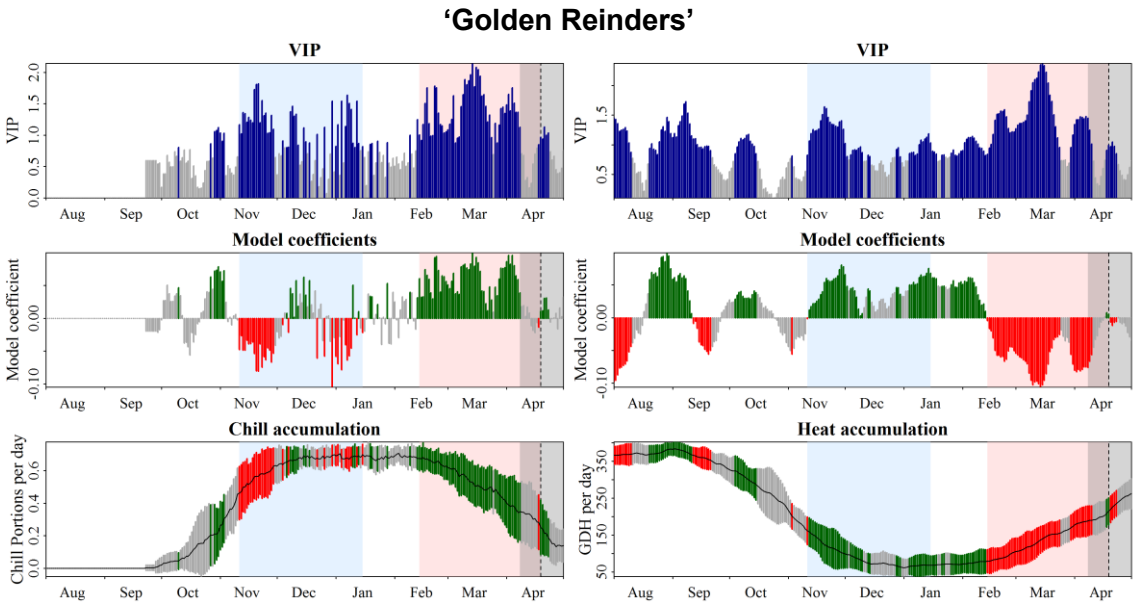

Figure S34. Results obtained from the PLS regression analysis between blooming dates and daily mean chill and heat accumulation for 'Golden Reinders' in Mas Badia using the Dynamic Model and the GDH Model. See caption in Figure S25 for full explanation.

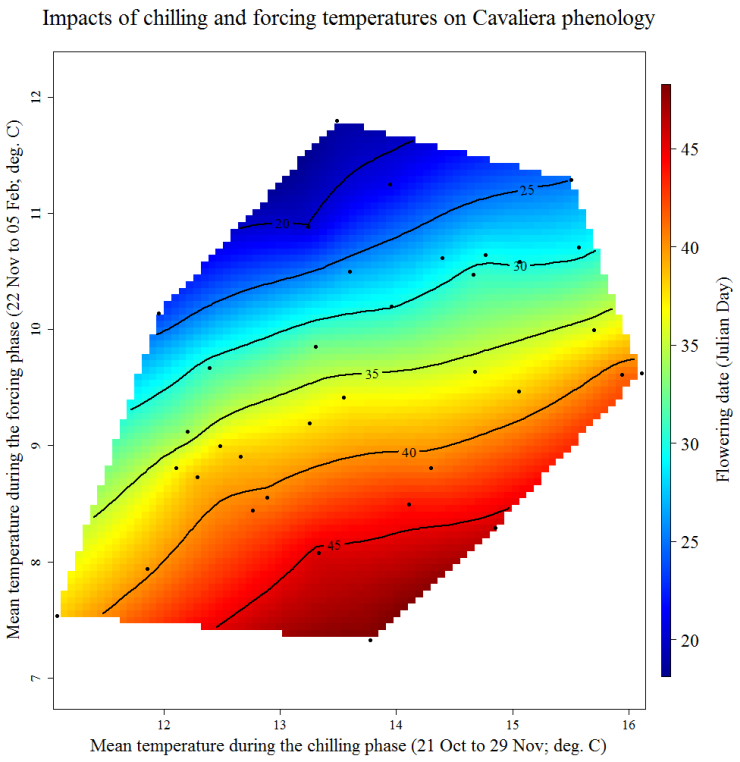

Figure S35. Response of 'Cavaliera' blooming dates to mean temperatures during the chilling and forcing phases in Mas de Bover. The colour spectrum has to be interpreted as variation of the flowering dates. Black dots represent the blooming dates recorded for the studied period (1979-2015). Although both axes start with different temperatures, they have the same scale.

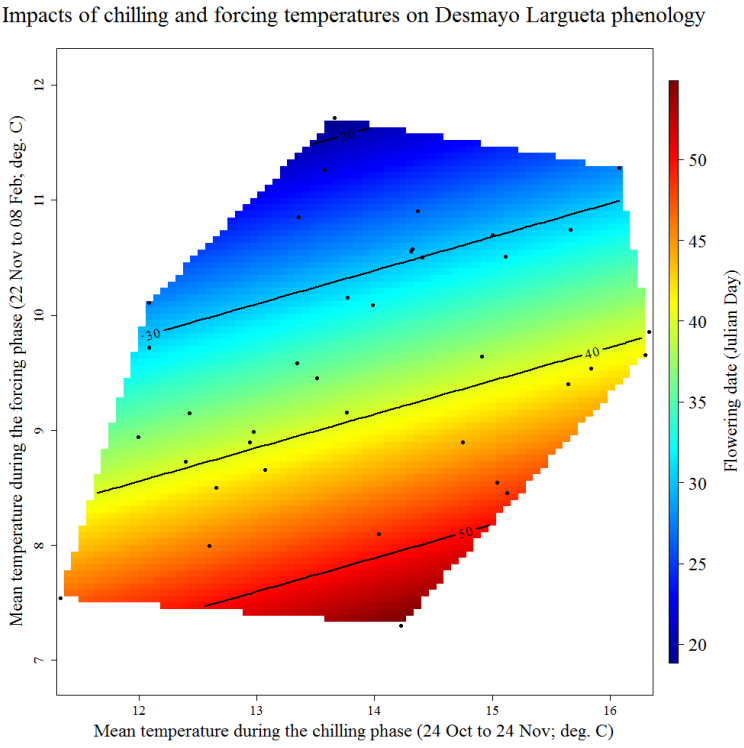

Figure S36. Response of 'Desmayo Largueta' blooming dates to mean temperatures during the chilling and forcing phases in Mas de Bover. See caption of Figure S35 for full explanation.

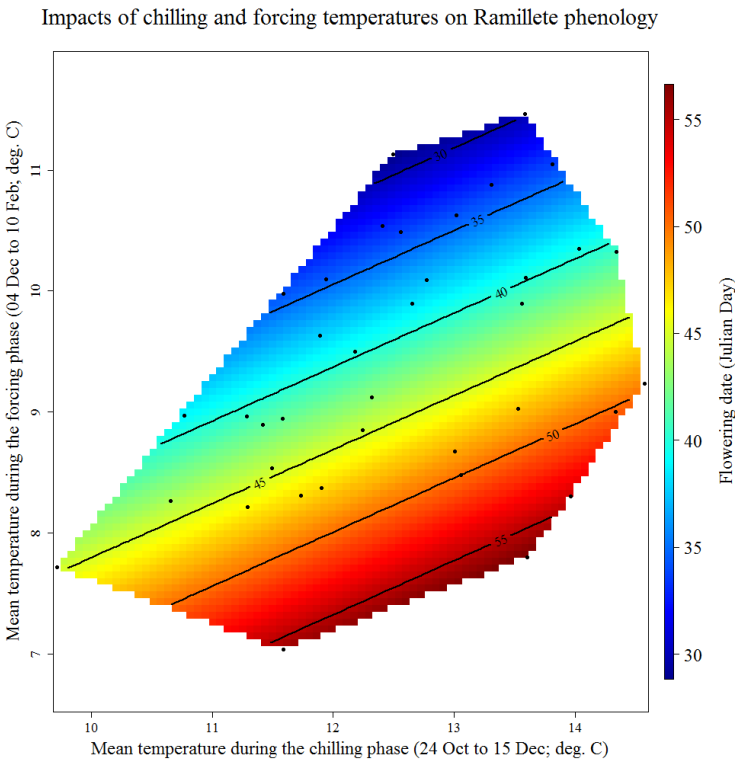

Figure S37. Response of 'Ramillete' blooming dates to mean temperatures during the chilling and forcing phases in Mas de Bover. See caption of Figure S35 for full explanation.

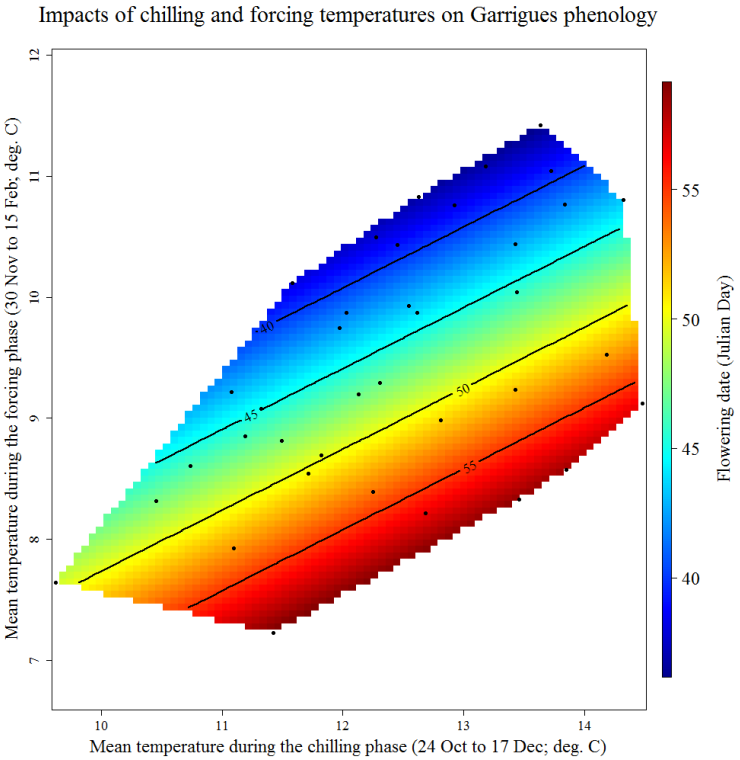

Figure S38. Response of 'Garrigues' blooming dates to mean temperatures during the chilling and forcing phases in Mas de Bover. See caption of Figure S35 for full explanation.

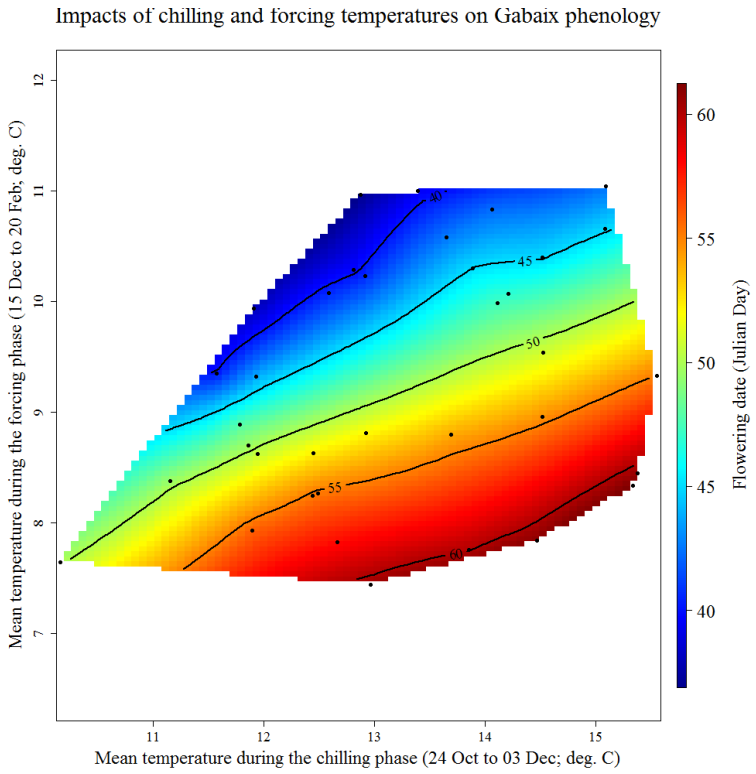

Figure S39. Response of 'Gabaix' blooming dates to mean temperatures during the chilling and forcing phases in Mas de Bover. See caption of Fig S35 for full explanation.

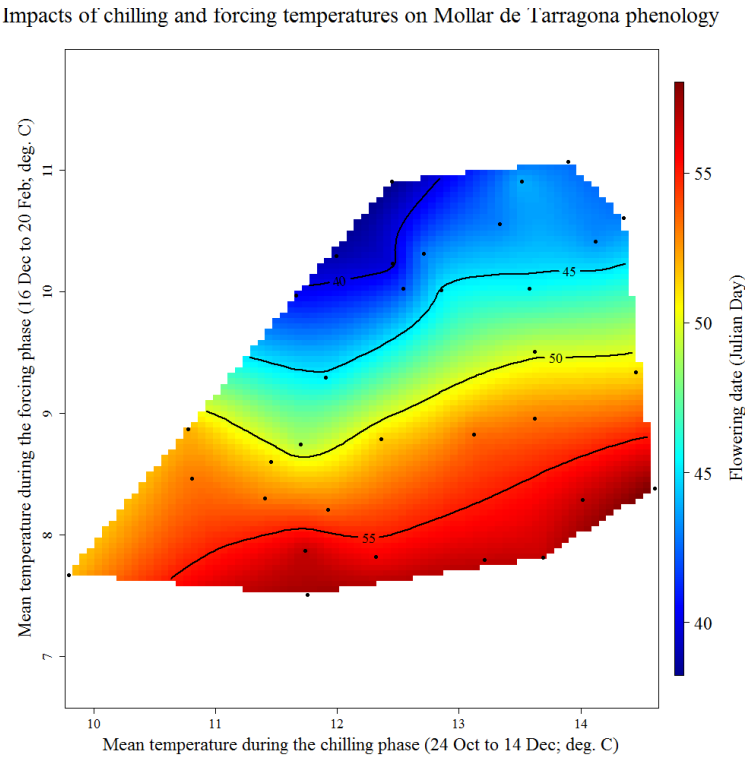

Figure S40. Response of 'Mollar de Tarragona' blooming dates to mean temperatures during the chilling and forcing phases in Mas de Bover. See caption of Fig S35 for full explanation.

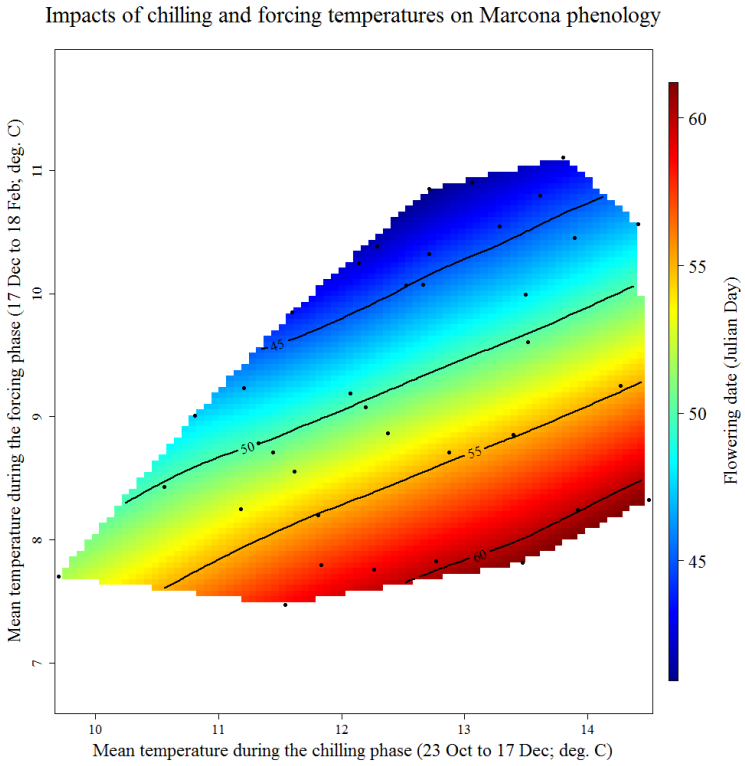

Figure S41. Response of 'Marcona' blooming dates to mean temperatures during the chilling and forcing phases in Mas de Bover. See caption of Fig S35 for full explanation.

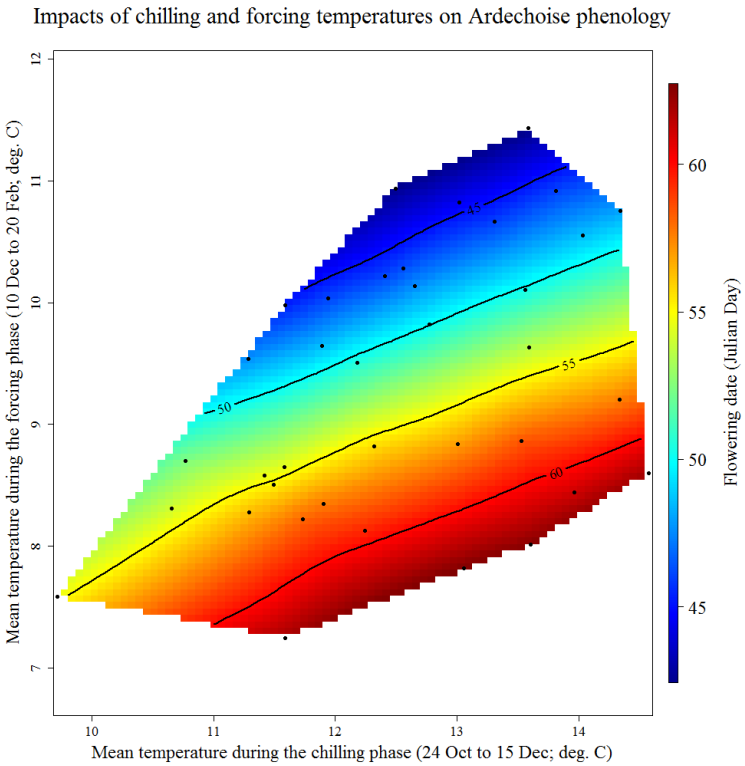

Figure S42. Response of 'Ardechoise' blooming dates to mean temperatures during the chilling and forcing phases in Mas de Bover. See caption of Figure S35 for full explanation.

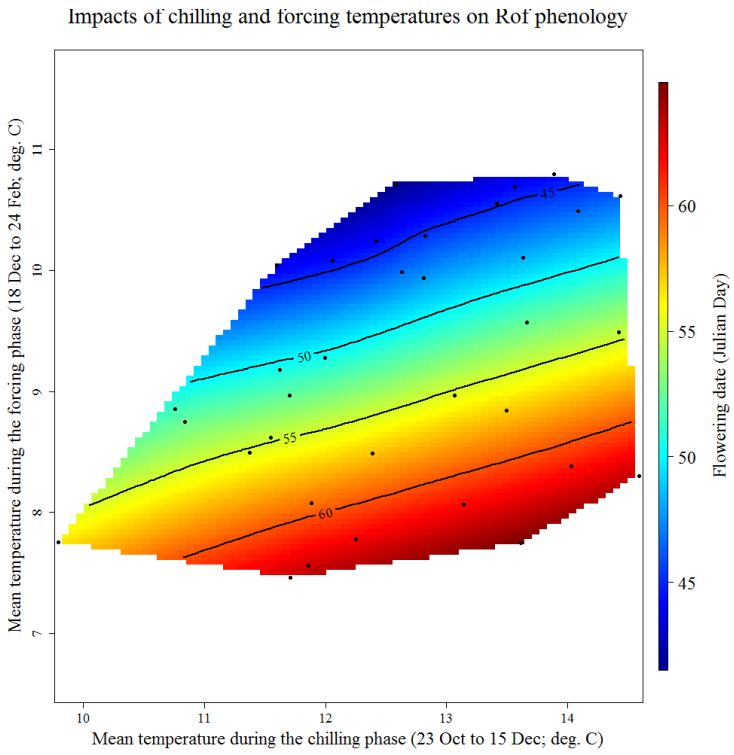

Figure S43. Response of 'Rof' blooming dates to mean temperatures during the chilling and forcing phases in Mas de Bover. See caption of Figure S35 for full explanation.

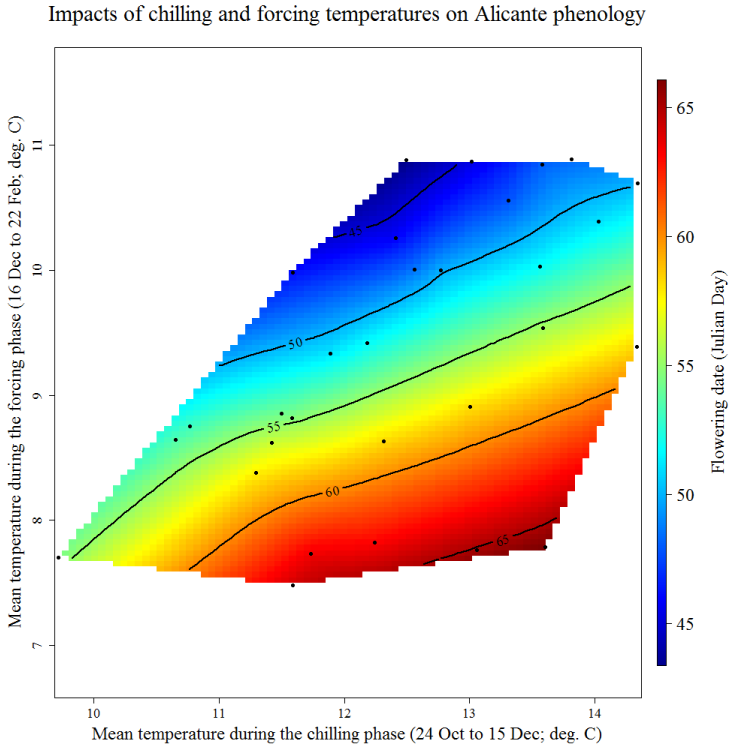

Figure S44. Response of 'Alicante' blooming dates to mean temperatures during the chilling and forcing phases in Mas de Bover. See caption of Figure S35 for full explanation.

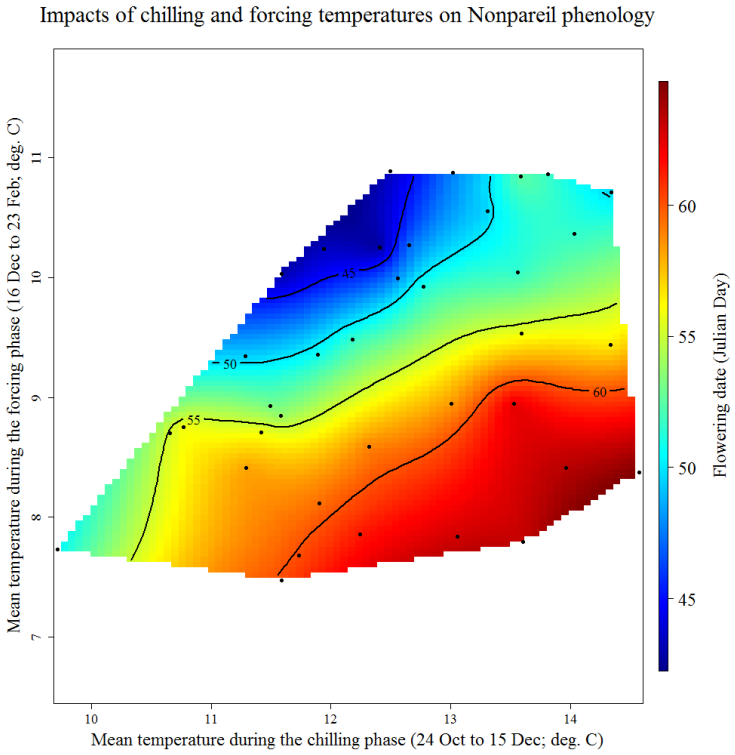

Figure S45. Response of 'Nonpareil' blooming dates to mean temperatures during the chilling and forcing phases in Mas de Bover. See caption of Figure S35 for full explanation.

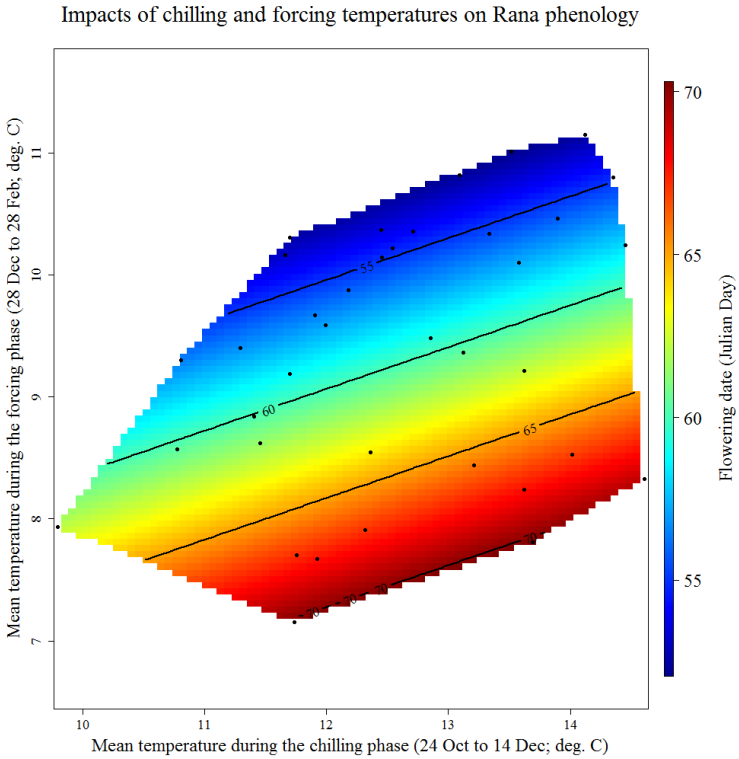

Figure S46. Response of 'Rana' blooming dates to mean temperatures during the chilling and forcing phases in Mas de Bover. See caption of Figure S35 for full explanation.

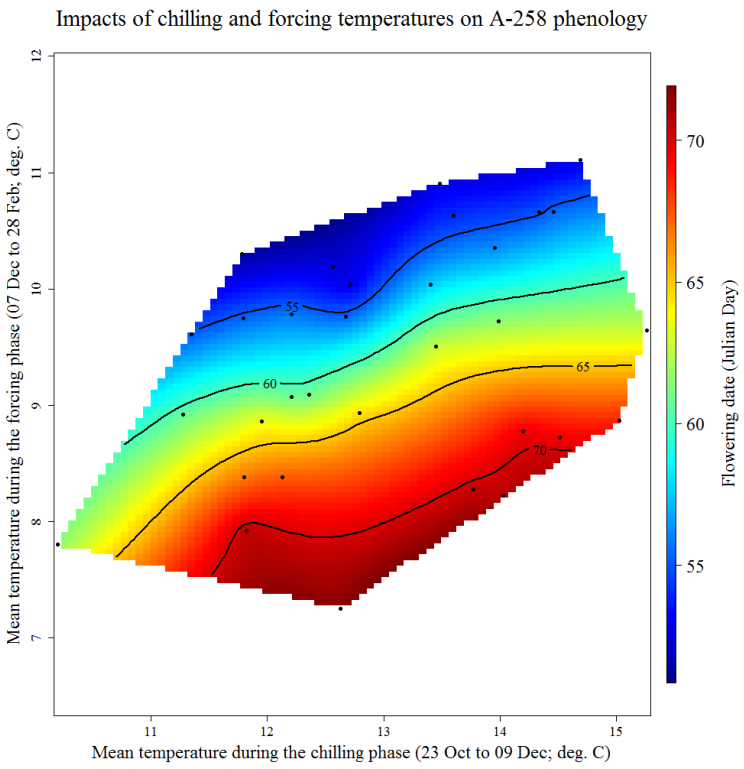

Figure S47. Response of 'A-258' blooming dates to mean temperatures during the chilling and forcing phases in Mas de Bover. See caption of Figure S35 for full explanation.

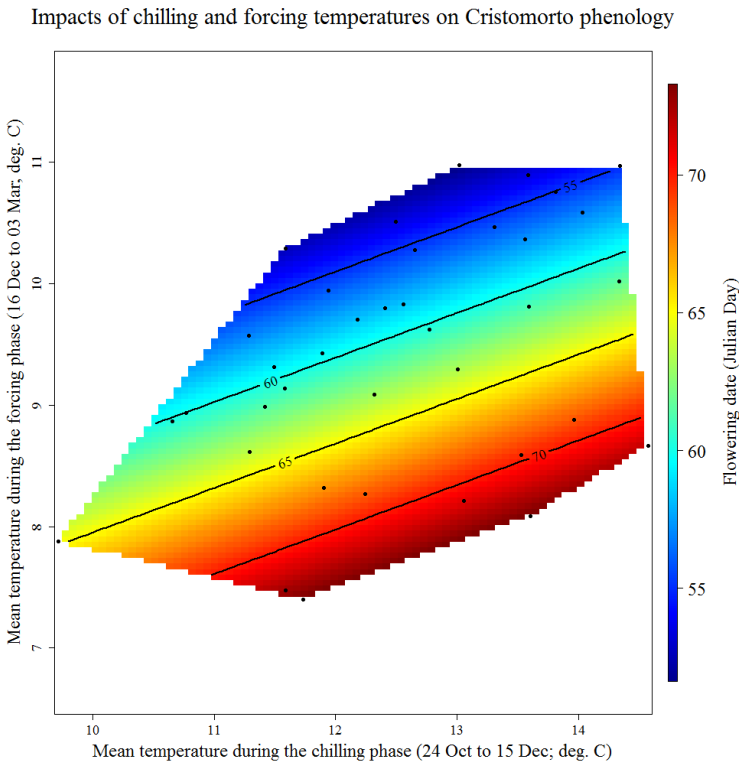

Figure S48. Response of 'Cristomorto' blooming dates to mean temperatures during the chilling and forcing phases in Mas de Bover. See caption of Figure S35 for full explanation.

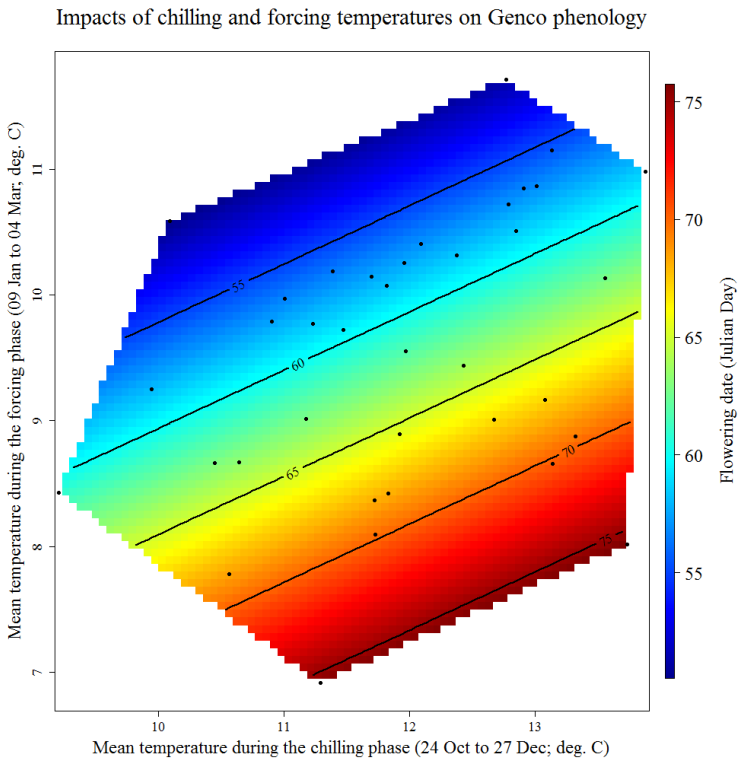

Figure S49. Response of 'Genco' blooming dates to mean temperatures during the chilling and forcing phases in Mas de Bover. See caption of Figure S35 for full explanation.

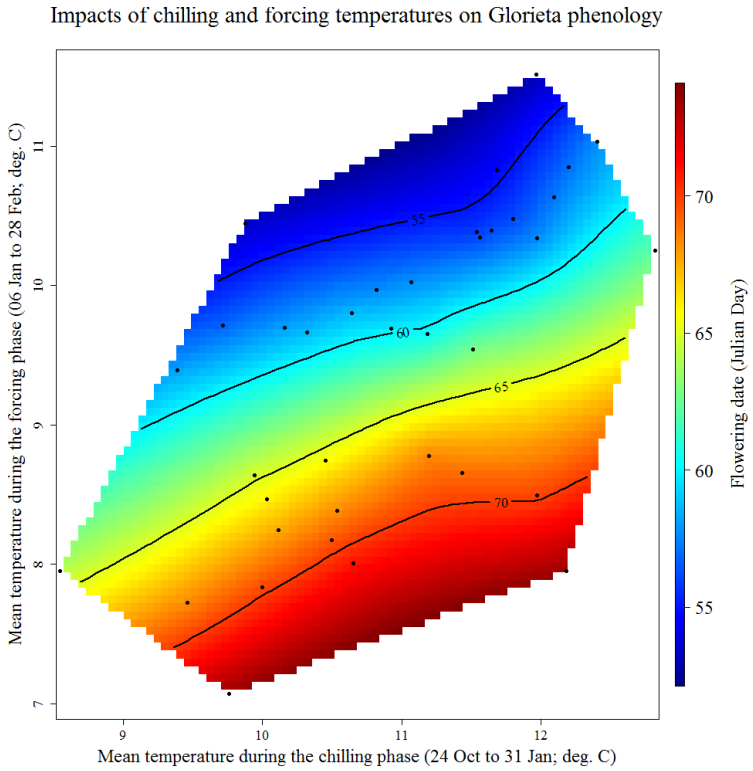

Figure S50. Response of 'Glorieta' blooming dates to mean temperatures during the chilling and forcing phases in Mas de Bover. See caption of Figure S35 for full explanation.

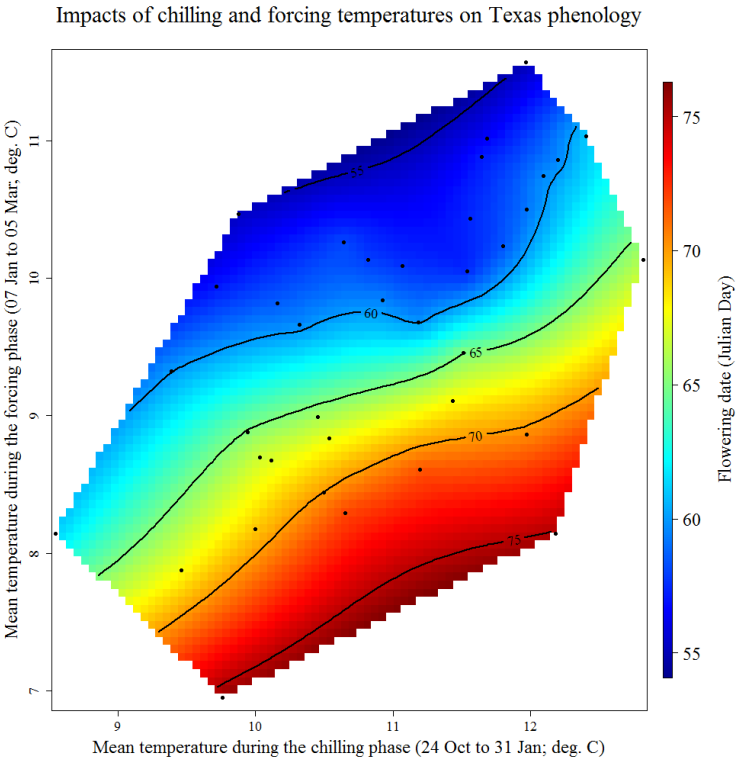

Figure S51. Response of 'Texas' blooming dates to mean temperatures during the chilling and forcing phases in Mas de Bover. See caption of Figure S35 for full explanation.

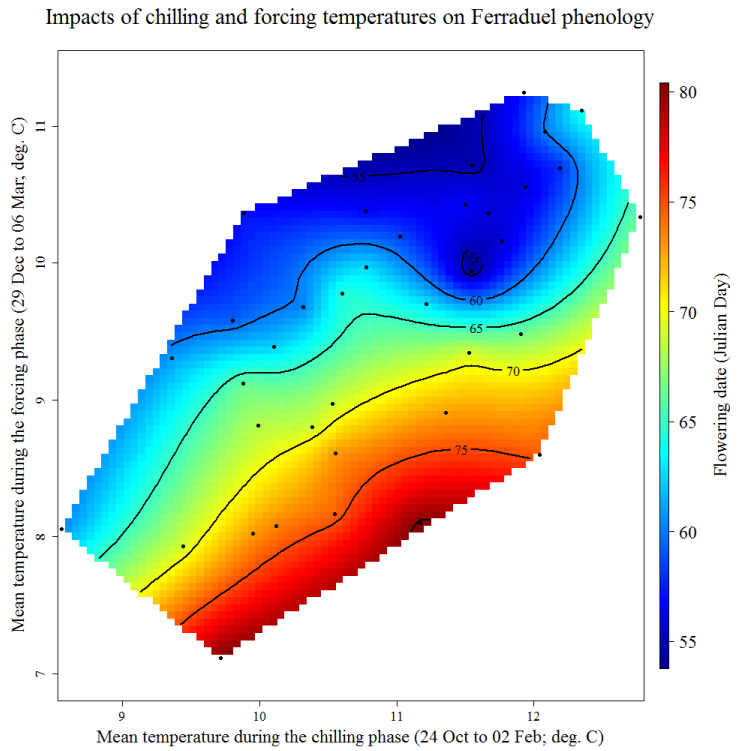

Figure S52. Response of 'Ferraduel' blooming dates to mean temperatures during the chilling and forcing phases in Mas de Bover. See caption of Figure S35 for full explanation.

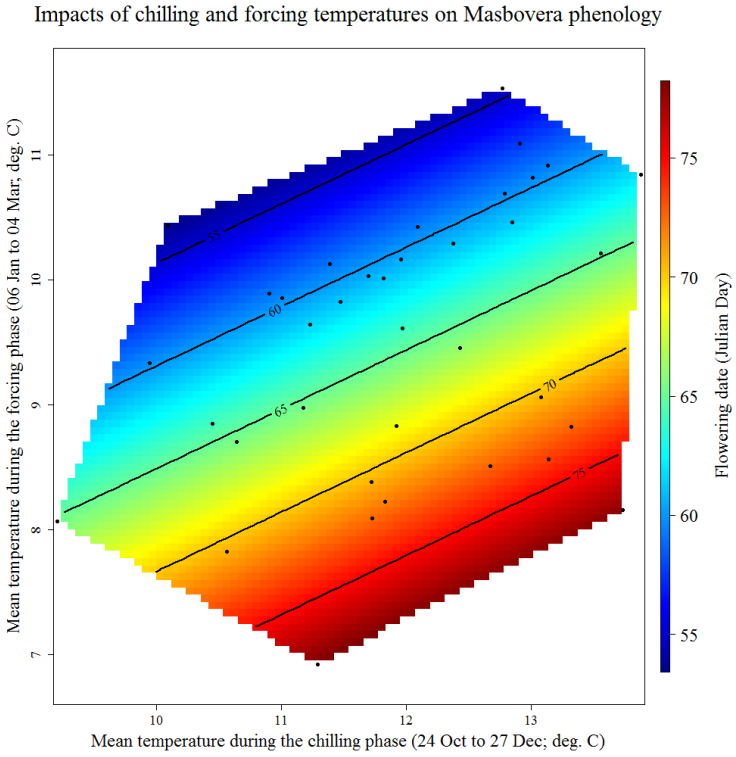

Figure S53. Response of 'Masbovera' blooming dates to mean temperatures during the chilling and forcing phases in Mas de Bover. See caption of Figure S35 for full explanation.

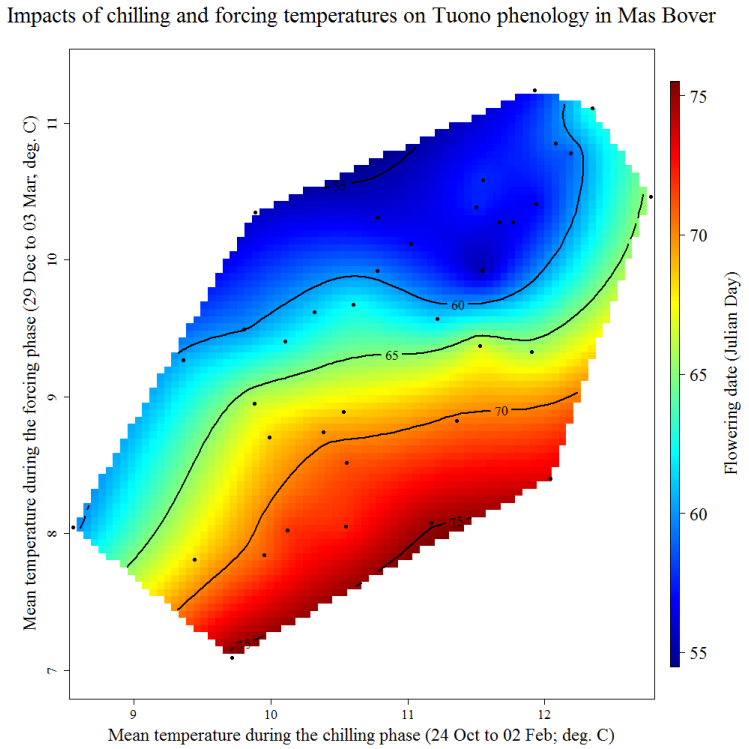

Figure S54. Response of 'Tuono' blooming dates to mean temperatures during the chilling and forcing phases in Mas de Bover. See caption of Figure S35 for full explanation.

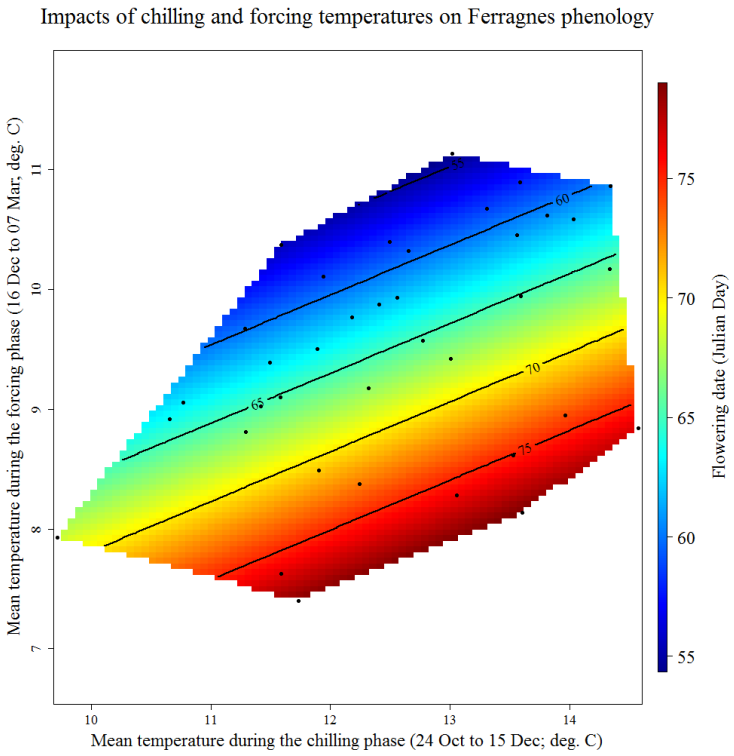

Figure S55. Response of 'Ferragnes' blooming dates to mean temperatures during the chilling and forcing phases in Mas de Bover. See caption of Figure S35 for full explanation.

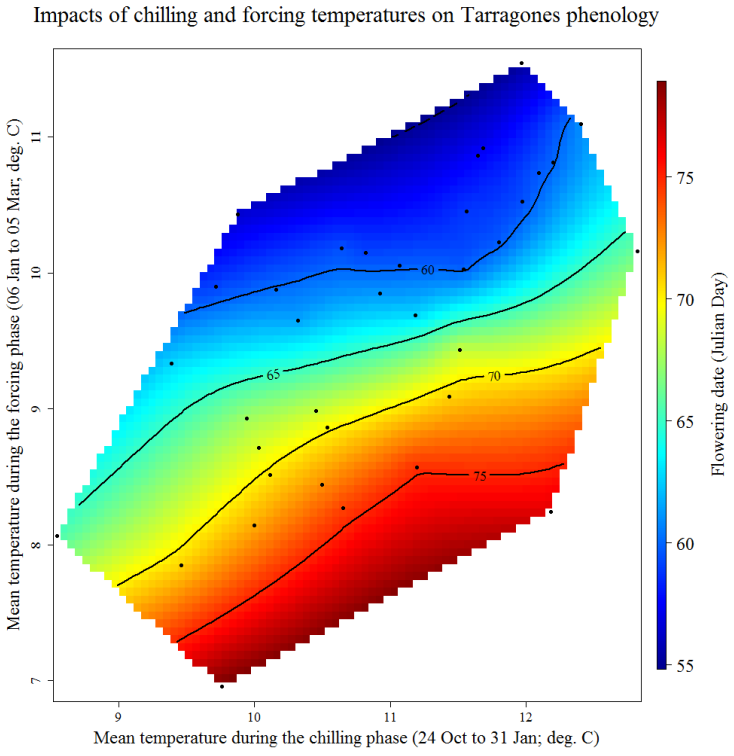

Figure S56. Response of 'Tarragonès' blooming dates to mean temperatures during the chilling and forcing phases in Mas de Bover. See caption of Figure S35 for full explanation.

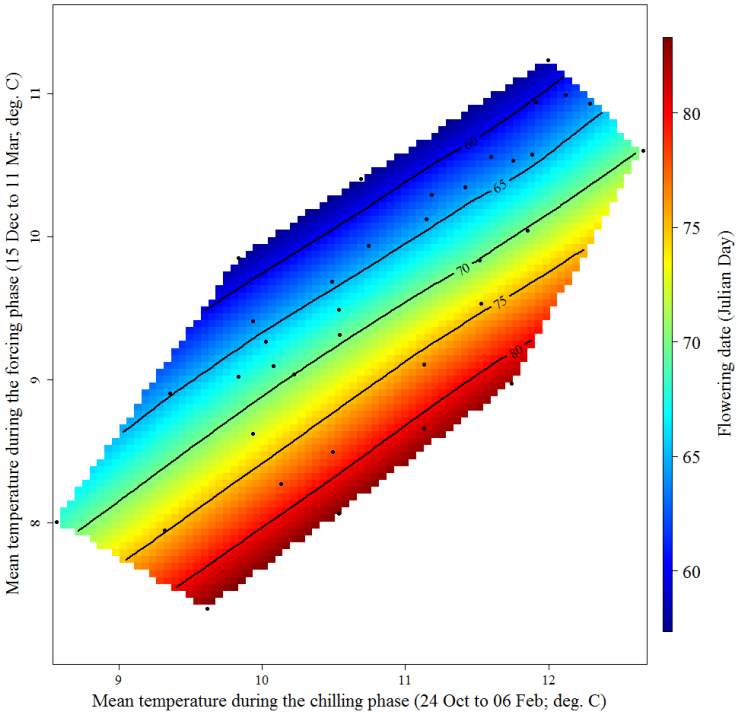

Figure S57. Response of 'Tardy Nonpareil' blooming dates to mean temperatures during the chilling and forcing phases in Mas de Bover. See caption of Figure S35 for full explanation.

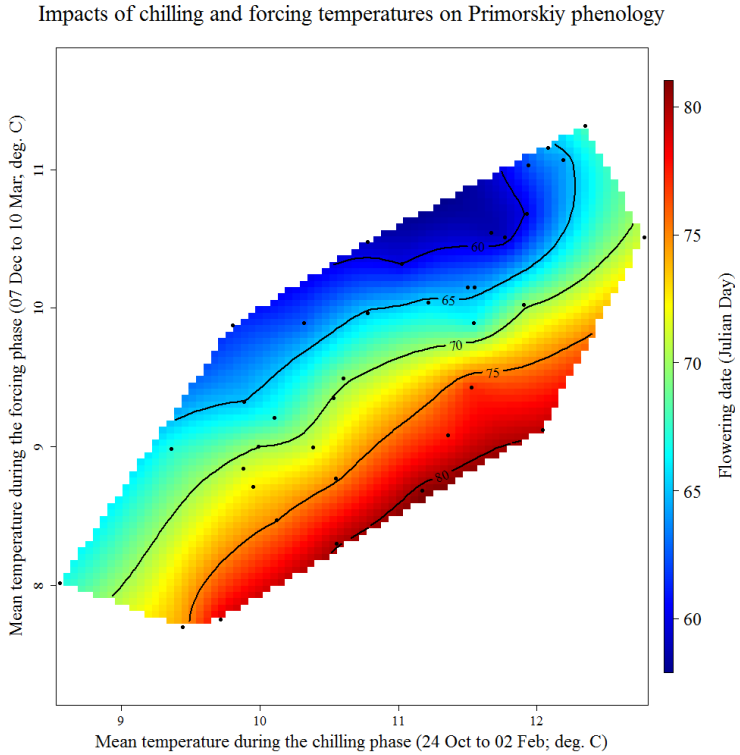

Figure S58. Response of 'Primorskiy' blooming dates to mean temperatures during the chilling and forcing phases in Mas de Bover. See caption of Figure S35 for full explanation.

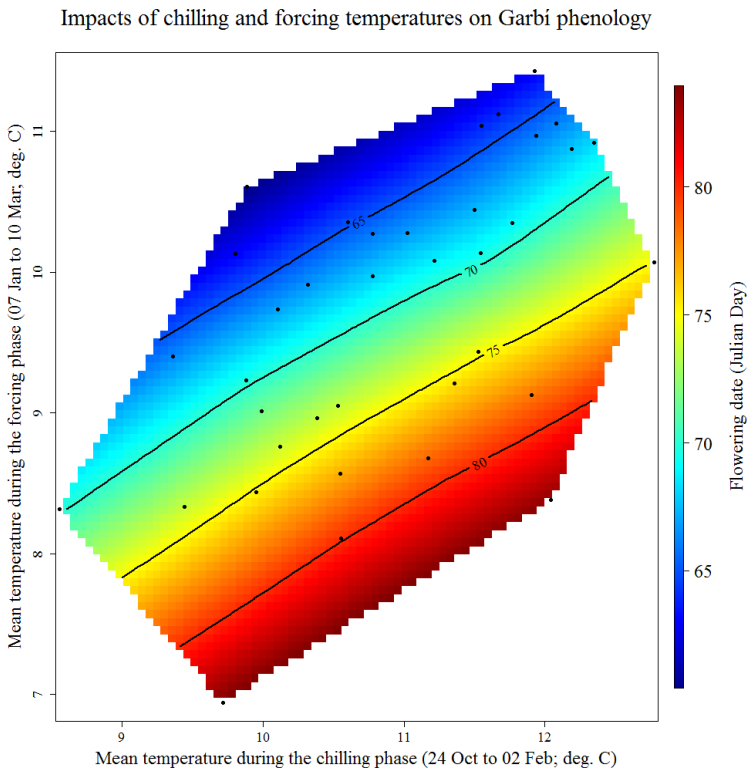

Figure S59. Response of 'Garbí' blooming dates to mean temperatures during the chilling and forcing phases in Mas de Bover. See caption of Figure S35 for full explanation.

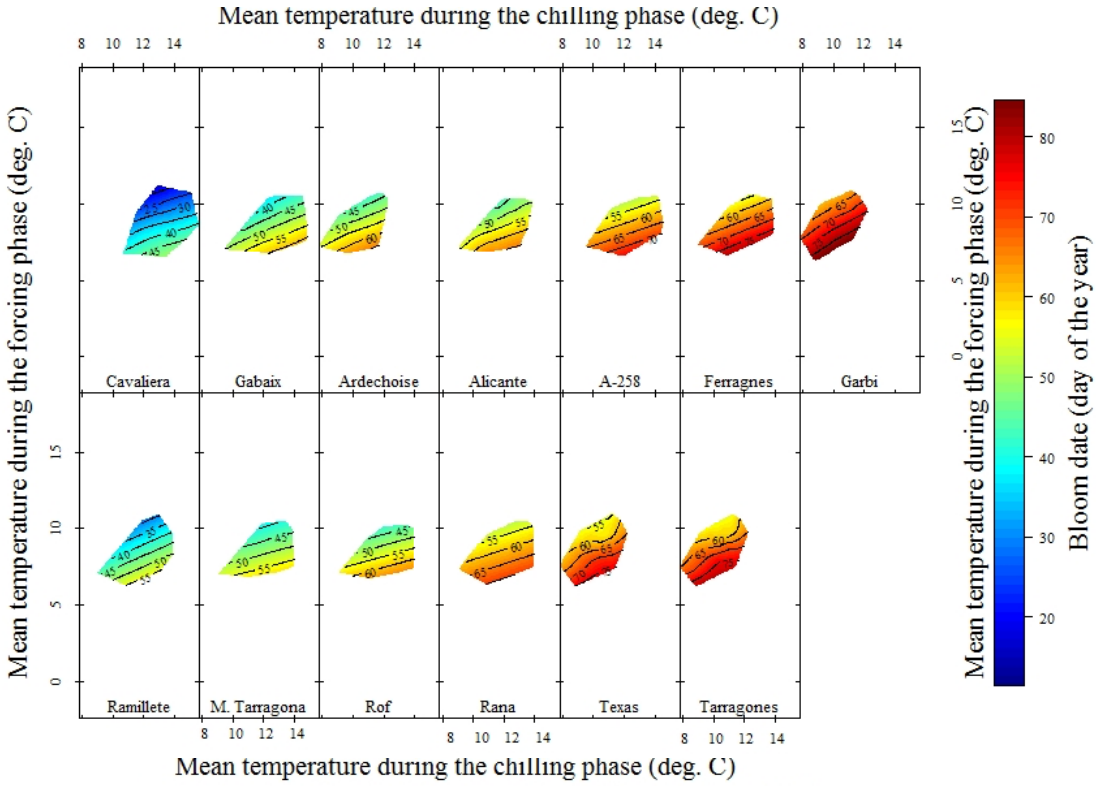

Figure S60. Response of blooming dates to mean temperatures during the chilling and forcing phases in Mas de Bover for 'Cavaliera', 'Gabaix', 'Ardechoise', 'Alicante', 'A-258', 'Ferragnes', 'Garbí', 'Ramillete', 'M.Tarragona', 'Rof', 'Rana', 'Texas' and 'Tarragones'. See caption of Figure S35 for full explanation.

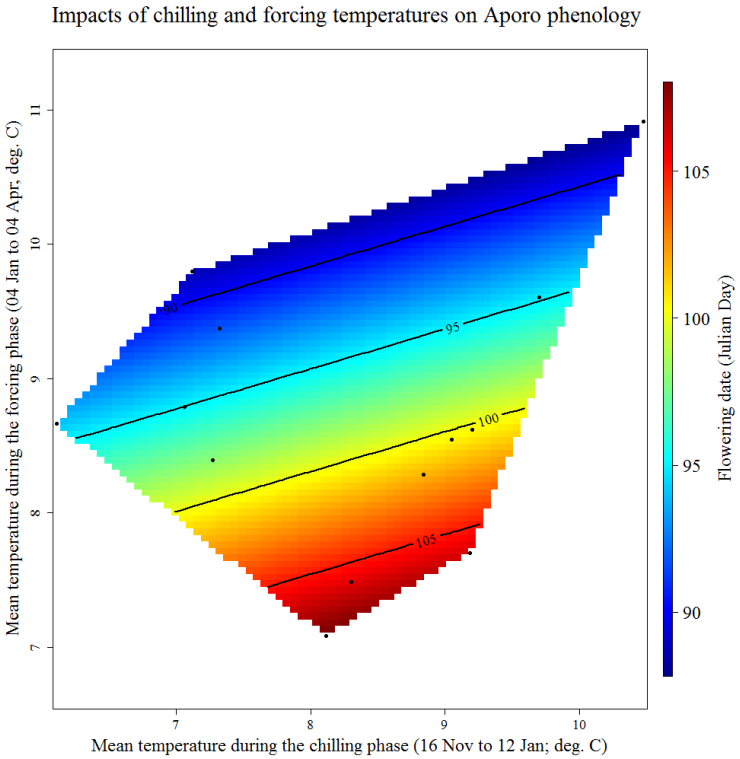

Figure S61. Response of 'Aporo' blooming dates to mean temperatures during the chilling and forcing phases in Mas Badia. The colour spectrum has to be interpreted as variation of the flowering dates. Black dots represent the blooming dates recorded for the studied period (1992-2018).

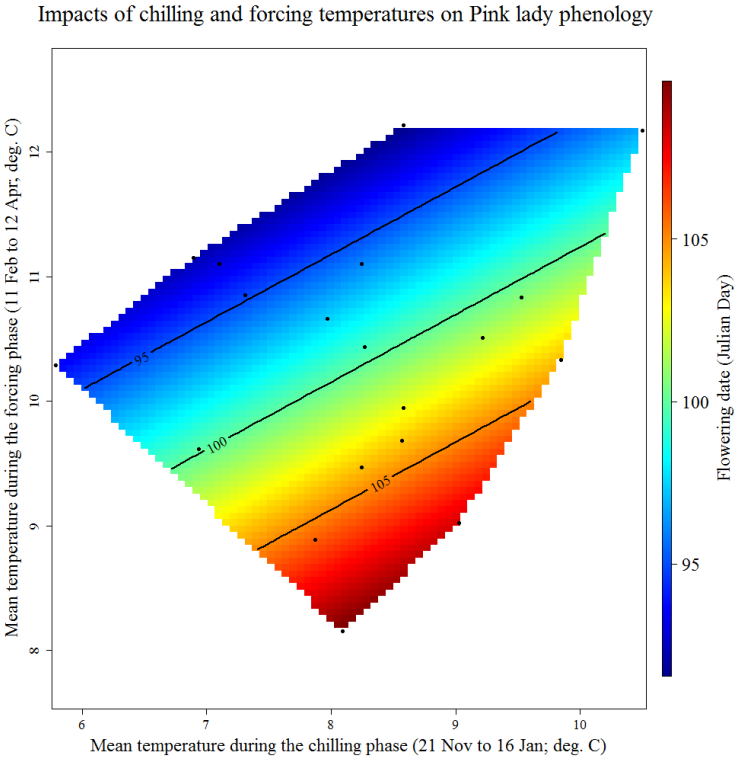

Figure S62. Response of 'Pink Lady' blooming dates to mean temperatures during the chilling and forcing phases in Mas Badia. See caption of Figure S61 for full explanation.

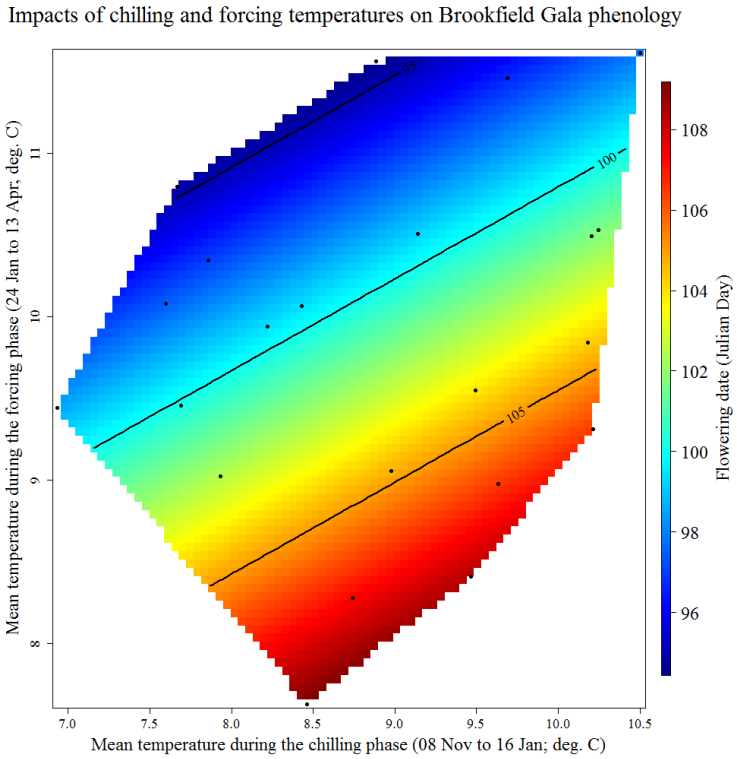

Figure S63. Response of 'Brookfield Gala' blooming dates to mean temperatures during the chilling and forcing phases in Mas Badia. See caption of Figure S61 for full explanation.

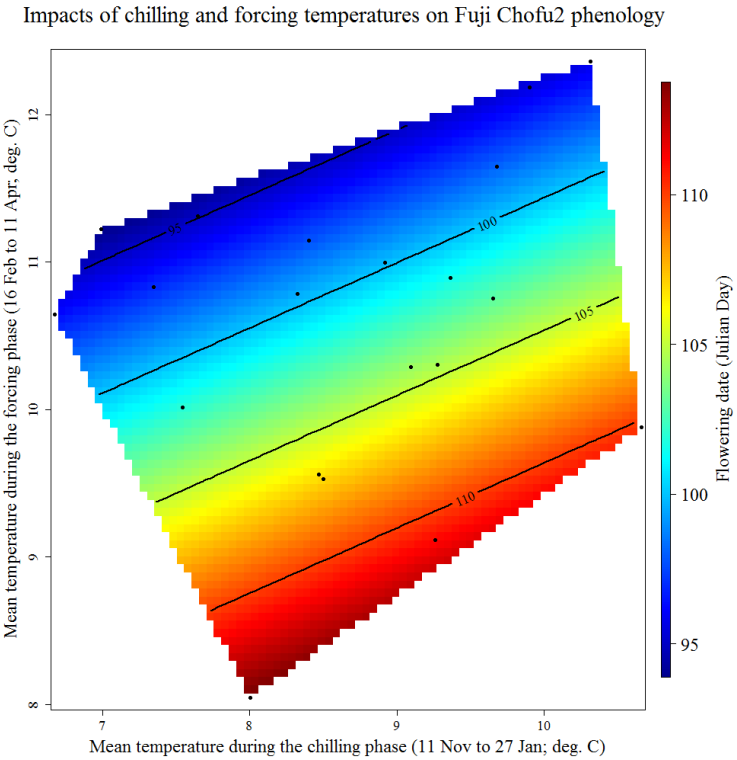

Figure S64. Response of 'Fuji Chofu 2' blooming dates to mean temperatures during the chilling and forcing phases in Mas Badia. See caption of Figure S61 for full explanation.

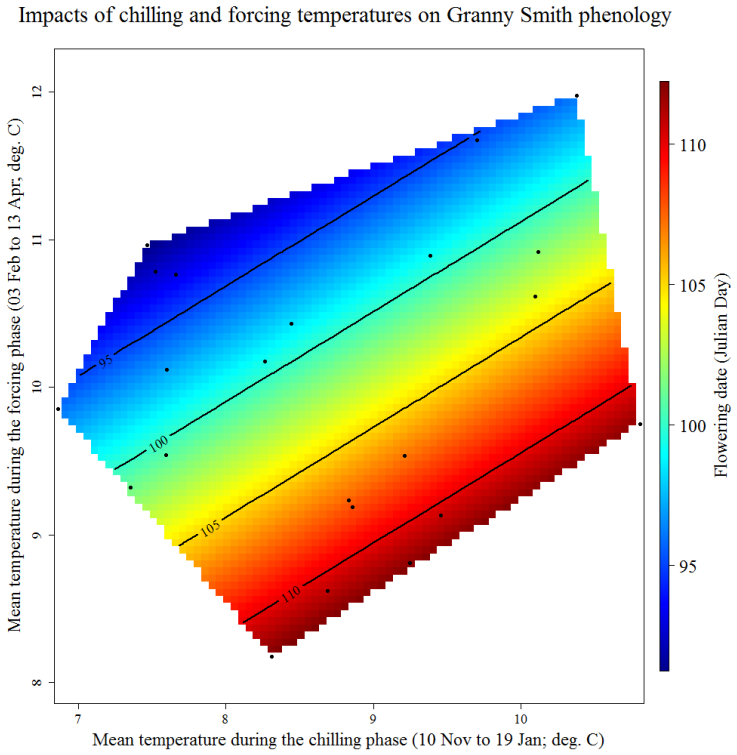

Figure S65. Response of 'Granny Smith' blooming dates to mean temperatures during the chilling and forcing phases in Mas Badia. See caption of Figure S61 for full explanation.

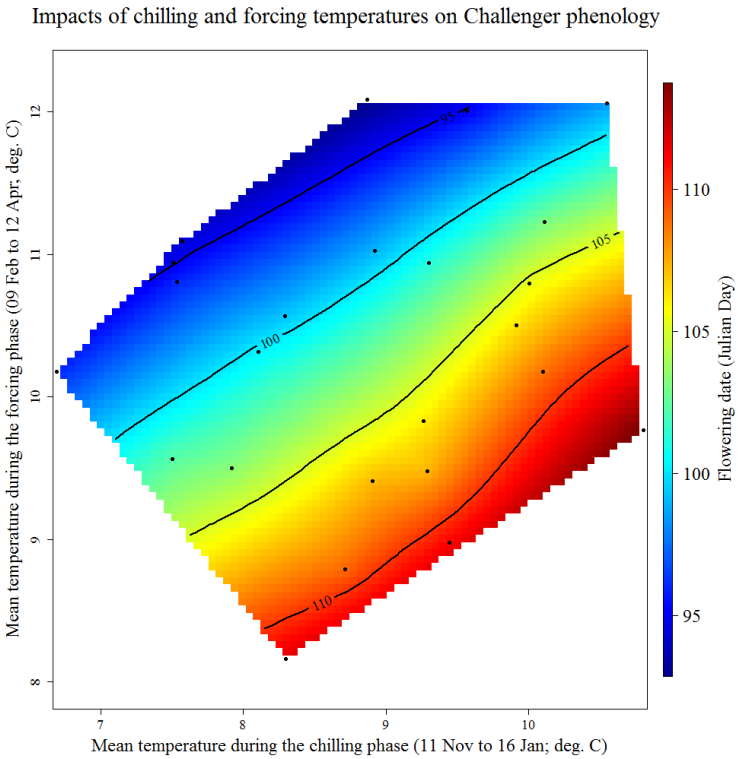

Figure S66. Response of 'Challenger' blooming dates to mean temperatures during the chilling and forcing phases in Mas Badia. See caption of Figure S61 for full explanation.

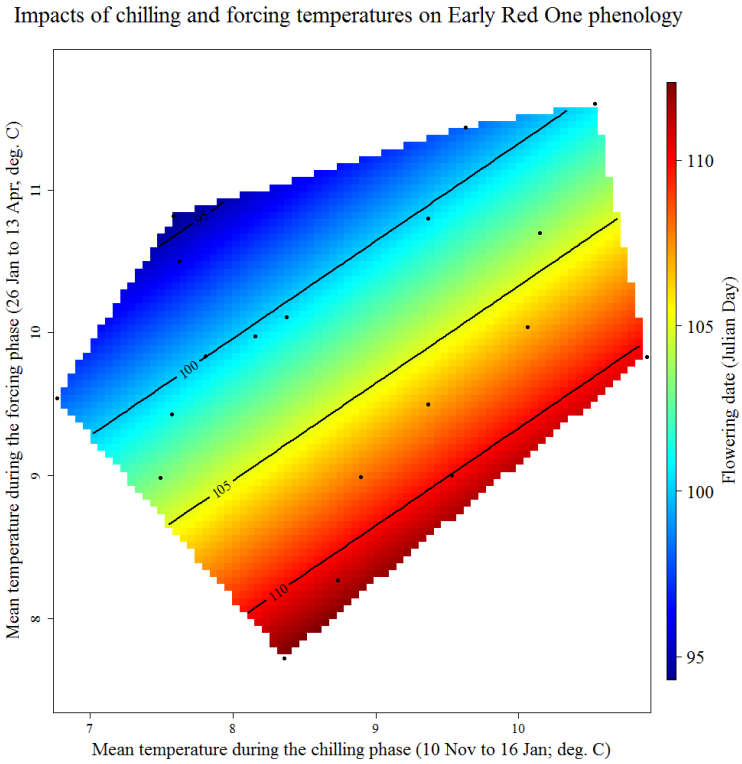

Figure S67. Response of 'Early Red One' blooming dates to mean temperatures during the chilling and forcing phases in Mas Badia. See caption of Figure S61 for full explanation.

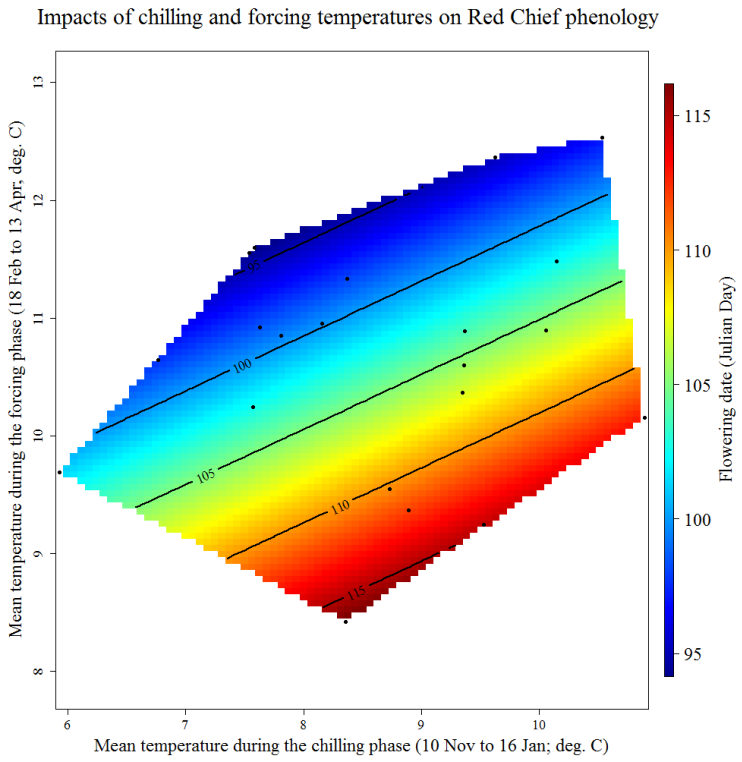

Figure S68. Response of 'Red Chief' blooming dates to mean temperatures during the chilling and forcing phases in Mas Badia. See caption of Figure S61 for full explanation.

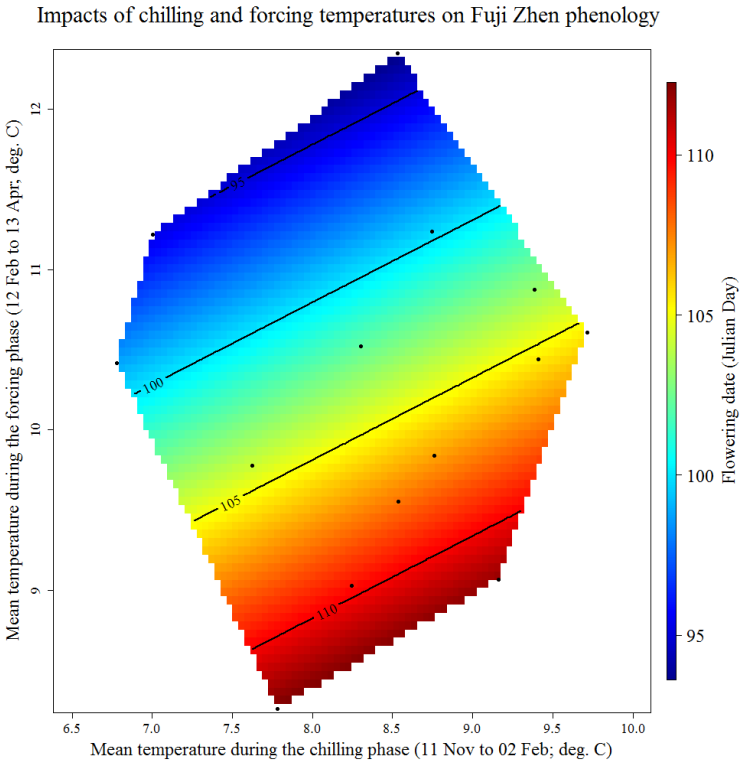

Figure S69. Response of 'Fuji Zhen' blooming dates to mean temperatures during the chilling and forcing phases in Mas Badia. See caption of Figure S61 for full explanation.

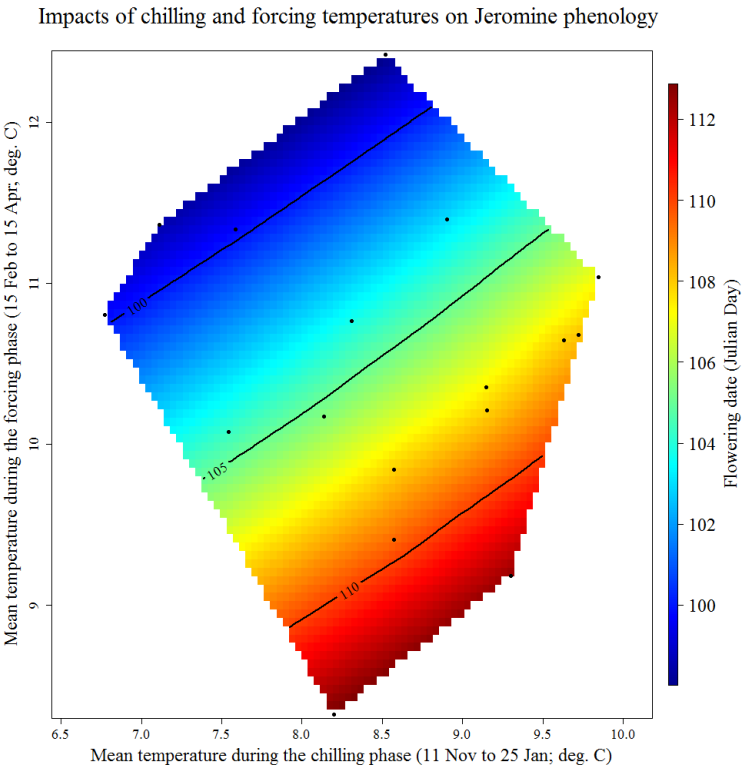

Figure S70. Response of 'Jeromine' blooming dates to mean temperatures during the chilling and forcing phases in Mas Badia. See caption of Figure S61 for full explanation.

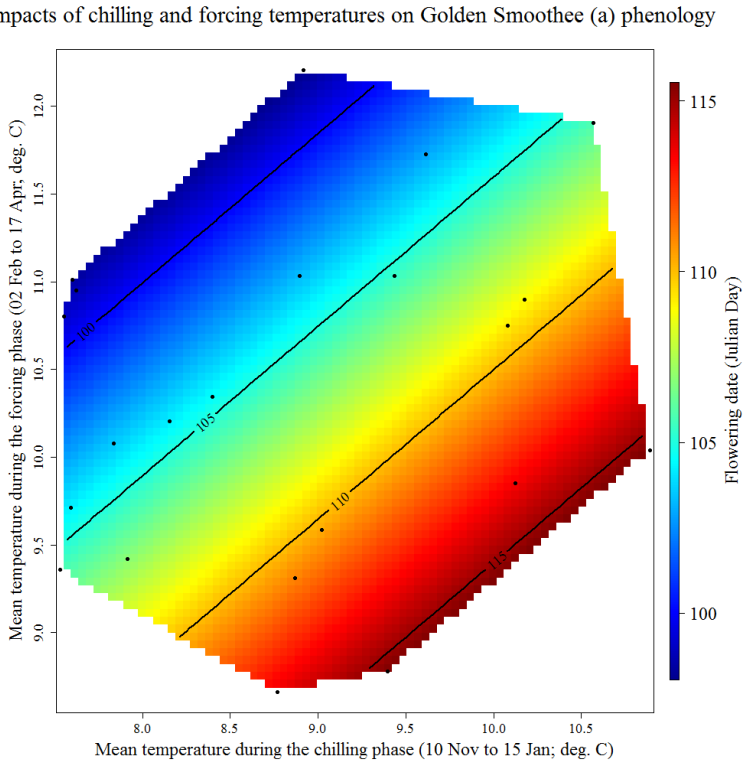

Figure S71. Response of 'Golden Smoothee' blooming dates to mean temperatures during the chilling and forcing phases in Mas Badia. See caption of Figure S61 for full explanation.

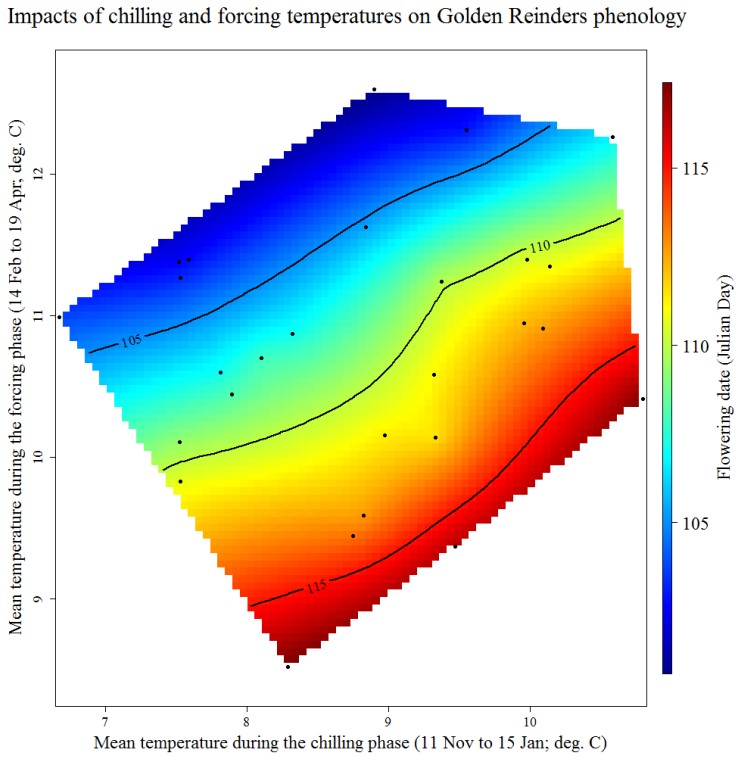

Figure S72. Response of 'Golden Reinders' blooming dates to mean temperatures during the chilling and forcing phases in Mas Badia. See caption of Figure S61 for full explanation.

Table S1. Temperature details during the phenological seasons in Mas Badia and Mas de Bover. Mean, maximum and minimum temperatures for each month, are calculated as the means for period 1978-2015 in Mas de Bover and 1992-2018 in Mas Badia.

		IRTA Mas de Bover			IRTA Mas Badia		
		T mean (ºC)	T min (ºC)	T max (ºC)	T mean (ºC)	T min (ºC)	T max (ºC)
	October	17.6	12.7	22.5	16.3	10.9	21.8
Autumn	November	12.7	7.8	17.6	11.4	5.7	17.0
	December	9.7	4.7	14.7	8.2	2.4	14.0
	January	9.0	3.9	14.1	7.7	1.8	13.5
Winter	February	9.8	4.6	14.9	8.1	2.2	14.0
	March	12.0	6.7	17.2	10.7	4.6	16.8
	April	13.9	8.7	19.1	13.2	7.3	19.2
Spring	May	17.2	12.1	22.3	17.0	11.1	22.8
	June	21.3	16.2	26.4	20.9	14.9	26.8
Annual		13.7	8.6	18.8	12.6	6.8	18.4

Table S2. Blooming past trends for 25 almond cultivars studied in Mas de Bover following the equation [Blooming date = Q*(data year – first data year) + B] where Q means the slope, B means the intercept of the equation, data year is the year for which blooming date is to be calculated, and first data year is 1979. n is the number of years of the dataset. Data available: year ranges of bloom data available for each cultivar. The presence of a statistically significant trend is evaluated using the Z value using the Mann-Kendall test. Levels of significance: NS: not significant; MS: marginally significant ($p<0.10$); * ($p<0.05$); **($p<0.01$); ***($p<0.001$).

Cultivars	Data available	First Year	Last Year	Test Z	Q	B	n	Sign.
Cavaliera	1979-1997; 2000-2015	1979	2015	-0.11	0.000	36.00	35	NS
Desmayo Largueta	1979-2015	1979	2015	0.81	0.123	36.57	37	NS
Ramillete	1979-2015	1979	2015	0.75	0.102	39	37	NS
Garrigues	1979-2015	1979	2015	0.20	0.000	46.00	37	NS
Gabaix	1979-1998; 2000-2015,	1979	2015	0.25	0.015	50.96	36	NS
Mollar de Tarragona	1979-1997; 2001-2015	1979	2015	0.62	0.065	49.065	34	NS
Marcona	1979-2015	1979	2015	0.20	0.000	49.00	37	NS
Ardechoise	1979-2015	1979	2015	0.69	0.082	48.61	37	NS
Rof	1979-1997; 2001-2015	1979	2015	0.04	0.000	55	34	NS
Alicante	1979-1991; 1994-1999; 2001-2011	1979	2011	0.48	0.083	52.08	30	NS
Nonpareil	1979-2015	1979	2015	-0.35	-0.047	55.233	37	NS
Rana	1979-2015	1979	2015	-0.98	-0.098	61.343	37	NS
A-258	1979-1980; 1984-1987; 1990-2015	1979	2015	0.26	0.000	59.00	32	NS
Cristomorto	1979-2015	1979	2015	-0.13	0.000	62.00	37	NS
Genco	1979-2015	1979	2015	0.00	0.000	63.00	37	NS
Glorieta	1979-2015	1979	2015	-0.56	-0.082	62.819	37	NS
Texas	1979-2015	1979	2015	-0.62	-0.111	66.111	37	NS
Ferraduel	1979-2015	1979	2015	-0.33	-0.056	66.11	37	NS
Masbovera	1979-2015	1979	2015	0.47	0.077	61.679	37	NS
Tuono	1979-2015	1979	2015	-0.66	-0.077	64.465	37	NS
Ferragnes	1979-2015	1979	2015	0.46	0.063	65.00	37	NS
Tarragones	1979-2002; 2004-2015	1979	2015	-0.27	0.000	64	36	NS
Tardy Nonpareil	1979-2006; 2008-2015	1979	2015	1.19	0.143	67.357	36	NS
Primorskiy	1979-2015	1979	2015	0.21	0.023	68.568	37	NS
Garbí	1979-2015	1979	2015	-0.72	-0.070	71.39	37	NS

Table S3. Blooming past trends for 12 apple cultivars studied in Mas Badia following the equation [Blooming date = Q*(data year – first data year) + B] where Q means the slope, B means the intercept of the equation, data year is the year for which blooming date is to be calculated, and first data year is the first data year of each bloom dataset. n is the number of years of dataset. The presence of a statistically significant trend is evaluated using the Z value using the Mann-Kendall test. Levels of significance: NS: not significant; MS: marginally significant (p<0.10); * (p<0.05); **(p<0.01); ***(p<0.001).

Cultivar	Data available	First year	Last year	Test Z	Q	B	n	Sig
Aporo	2000-2013	2000	2013	1.10	0.500	87.00	13	NS
Pink Lady	1999-2017	1999	2017	-0.77	-0.182	104.91	19	NS
Brookfield Gala	1997-2018	1997	2018	0.82	0.200	97.60	22	NS
Fuji Chofu2	1995-2013	1995	2013	0.49	0.174	97.54	19	NS
Granny Smith	1992-2013	1992	2013	0.31	0.100	100.85	22	NS
Challenger	1995-2018	1995	2018	0.00	0.000	102.00	24	NS
Early Red One	1992-2010	1992	2010	0.70	0.267	100.20	19	NS
Red Chief	1992-2012	1992	2012	0.09	0.000	103.00	21	NS
Fuji Zhen	2004-2017	2004	2017	-1.21	-0.500	111.25	14	NS
Jeromine	2002-2018	2002	2018	-0.75	-0.310	110.40	17	NS
Golden Smoothee	1992-2002; 2008-2013	1992	2018	0.79	0.167	105.50	16	NS
Golden Reinders	1992-2018	1992	2018	-0.31	-0.040	109.24	27	NS

Table S4. Temperature past trends for the studied period in Reus Airport W.S (1978-2015) and La Tallada W.S following the equation [Temperature = Q*(data year – first data year) + B] where Q means the slope. B means the intercept of the equation, data year is the year for which temperature is to be calculated, and first data year is 1978 in Reus Airport and 1991 in La Tallada d'Empordà. The presence of a statistically significant trend is evaluated with the Z value using the Mann-Kendall test. Levels of significance: NS: not significant; MS: marginally significant (p<0.10); * (p<0.05); **(p<0.01); ***(p<0.001).

W.S	Time series	Test Z	Q	B	Signific
Reus Airport	Maximum	4.28	0.050	20.40	***
	Minimum	0.12	0.002	11.15	NS
	Mean	2.66	0.026	15.79	**
La Tallada	Maximum	1.64	0.030	20.52	NS
	Minimum	-0.89	0.015	9.50	NS
	Mean	0.41	0,070	15.01	NS

Table S5. Analisis of Variance and Duncan's multiple range test for bloom date of almond blooming groups. DOY means Day of Year. N is the number of cultivars in each blooming group. Means with the same letter are not significantly different.

Sum of Squares	Mean Square	F Value	Pr > F	Duncan Grouping	Mean bloom date (DOY)	N	Blooming group
1959.58	653.19	36.78	<.0001	A	69	2	Extra late-blooming
				A	64	9	Late-Blooming
				B	55	9	Mid-blooming
				C	42	5	Early-blooming

Table S6. Analysis of Variance and Duncan's multiple range test for blooming date (DOY, day of the year) of the 25 almond cultivars. N is the number years for each cultivar. Means with the same letter are not significantly different. Alpha is 0.05

Sum of Squares	Mean Square	F Value	Pr > F	Cultivar	Mean Blooming date	N	Duncan Grouping
85437	3559.9	51.44	<.0001	'Garbi'	71	37	A
				'Primorskiy'	69	37	A B
				'Tardy Nonpareil'	68	36	A B
				'Ferragnes'	65	37	B C
				'Tarragones'	65	36	B C D
				'Masbovera'	64	37	B C D
				'Ferraduel'	64	37	B C D
				'Tuono'	64	37	C D E
				'Texas'	63	37	C D E
				'Glorieta'	62	37	C D E
				'Genco'	62	37	C D E
				'Cristomorto'	61	37	C D E
				'A-258'	61	32	D E
				'Rana'	60	37	E
				'Nonpareil'	54	37	F
				'Alicante'	54	30	F
				'Ardechoise'	53	37	F G
				'Rof'	53	34	F G
				'Marcona'	50	37	F G H
				'Gabaix'	49	36	G H
				'Mollar de Tarragona'	49	34	G H
				'Garrigues'	46	37	H
				'Ramillete'	42	37	I
				'Desmayo Largueta'	36	37	J
				'Cavaliera'	35	35	J

Table S7. Analysis of Variance and Duncan's multiple range test for blooming date (DOY; day of the year) of the 12 apple cultivars. N is the number years for each cultivar. Means with the same letter are not significantly different. Alpha is 0.05

Sum of Squares	Mean Square	F Value	Pr > F	Cultivar	Duncan Grouping	Mean	N
1981.9	180.2	4.00	<.0001	Golden Reinders	A	109	27
				Golden Smothee	A B	106	22
				Jeromine	A B	105	17
				Fuji Zhen	B C	104	14
				Early Red One	B C	103	19
				Red Chief	B C	103	21
				Challenger	B C D	103	24
				Grannny Smith	B C D	102	22
				Fuji Chofu2	B C D	102	20
				Brookfield Gala	B C D	101	22
				Pink Lady	C D	100	19
				Aporo	D	98	13

Table S8. Analysis of Variance and Duncan's multiple range test for bloom date of almond blooming groups plus apple cultivars. N is the number of cultivars in each blooming group. Means with the same letter are not significantly different. Aplha is 0.05. DOY is day of the year.

Sum of Squares	Mean Square	F Value	Pr > F	Duncan Grouping	Mean bloom date (DOY)	N	Blooming group
19295.8	4824.0	333.42	<.0001	A	103	12	Apple cultivars
				B	69	2	Extra late-Blooming (almond)
				B	64	9	Late-blooming (almond)
				C	55	9	Mid-blooming (almond)
				D	42	5	Early-blooming (almond)

Table S9. Analysis of Variance and Duncan's multiple range test for chill requirements (CR) in chill portion (CP) of almond blooming groups. N is the number of cultivars in each blooming group. Means with the same letter are not significantly different. Alpha is 0.05

Sum of Squares	Mean Square	F Value	Pr > F	Duncan Grouping	Mean CR (CP)	N	Blooming group
4146.126993	1382.042331	13.44	<.0001	A	54.13	2	Extra late-blooming
				A	42.18	9	Late-Blooming
				B	20.97	9	Mid-blooming
				B	16.47	5	Early-blooming

Table S10. Analysis of Variance and Duncan's multiple range test for heat requirements (HR) in growing degree hours (GDH) of almond blooming groups. N is the number of cultivars in each blooming group. Means with the same letter are not significantly different. Alpha is 0.05

Sum of Squares	Mean Square	F Value	Pr > F	Duncan Grouping	Mean HR (GDH)	N	Blooming group
3755621.85	1251873.95	0.99	0.4166	A	8242.0	2	Extra late-blooming
				A	7554.8	5	Early-Blooming
				A	7368.1	9	Late-blooming
				A	6876.4	9	Mid-blooming